

Aus dem Department für Diagnostische Labormedizin der
Universität Tübingen

Institut für Pathologie und Neuropathologie
Abteilung Allgemeine und Molekulare Pathologie und
Pathologische Anatomie

**Clonal Haematopoiesis in Patients with
angioimmunoblastic T-Cell Lymphoma**

**Inaugural-Dissertation
zur Erlangung des Doktorgrades
der Medizin**

**der Medizinischen Fakultät
der Eberhard Karls Universität
zu Tübingen**

vorgelegt von

Harland, Lennart Frank, geb. Fiedler

2021

Dekan: Professor Dr. B. Pichler

1. Berichterstatter: Professorin Dr. L. Quintanilla Martinez de Fend

2. Berichterstatter: Professorin Dr. J. Skokowa, Ph.D.

Tag der Disputation: 11.10.2021

Meinen Eltern

Table of Contents

I. Figures	4
II. Tables	5
III. Abbreviations	6
1 Introduction	8
1.1 The Impact and Systematic of lymphatic Malignancies	8
1.2 Angioimmunoblastic T-Cell Lymphoma (AITL)	10
1.2.1 Epidemiology	10
1.2.2 Clinical Significance	11
1.2.3 Tumour Biology and Pathology	12
1.3 Genetic Profile of AITL	14
1.3.1 Frequent genetic Alterations	14
1.3.2 RHOA	15
1.3.3 IDH2	16
1.3.4 TET2	17
1.3.5 DNMT3A	19
1.4 Clonal Haematopoiesis of indeterminate Potential	21
1.5 Aim of the Thesis	22
2 Material and Methods	23
2.1 Materials	23
2.1.1 Patient samples	23
2.1.2 Chemicals and Reagents	23
2.1.3 Kits	24
2.1.4 Consumable supplies	24
2.1.5 Oligonucleotide Sequences	24
2.1.6 Devices	25
2.1.7 Software	25
2.1.8 Companies	26
2.2 Study Design	27
2.3 Microscopy	28
2.4 DNA Extraction	28

2.5	DNA Quality Assessment	28
2.5.1	Polymerase Chain Reaction	28
2.5.2	Gel Electrophoresis	29
2.5.3	DNA Repair	30
2.6	Ion Torrent™ Next-Generation Sequencing	30
2.6.1	AITL Panel	30
2.6.2	MDS Panel	31
2.6.3	Generation of Amplicon Libraries.....	32
2.6.4	Quantification of Amplicon Libraries	33
2.6.5	Chip Loading and Sequencing.....	33
2.6.6	Genetic Analysis	34
2.6.7	Single Amplicon Validation	34
2.7	Blood Count	34
2.8	Statistical Analysis.....	35
3	Results	36
3.1	Patient Characteristics	36
3.2	Evaluation of Bone Marrow Quality	37
3.2.1	Microscopy	37
3.2.2	DNA Integrity	39
3.2.3	Final Sample Selection	40
3.3	Molecular Analysis	42
3.3.1	Quality of Next-Generation Sequencing	42
3.3.2	Genetic Findings.....	44
3.3.3	<i>TET2</i> Mutations	49
3.3.4	<i>DNMT3A</i> Mutations	51
3.4	Examination of Germline Variants.....	53
3.5	Examination of MDS Properties	54
3.5.1	Blood Count.....	54
3.5.2	Successive Molecular Analysis.....	57
4	Discussion.....	59
4.1	Patient Collective	59
4.1.1	Characteristics.....	59

4.1.2	Sample Quality	59
4.1.3	Bone Marrow Infiltration	60
4.2	Molecular Analysis	61
4.2.1	RHOA	61
4.2.2	IDH2	61
4.2.3	<i>TET2</i> and <i>DNMT3A</i> mediated Clonal Haematopoiesis.....	62
4.2.4	Germline Variants	64
4.3	Examination of MDS Properties	65
4.3.1	Blood Counts	65
4.3.2	Genetic Analysis	65
4.3.3	Divergent Evolution of AITL and MDS	67
4.4	Conclusion	69
4.5	Outlook.....	70
5	Summary.....	71
5.1	Summary (English).....	71
5.2	Zusammenfassung (Deutsch)	73
6	References.....	75
7	Declaration of Authorship.....	85
8	Acknowledgements	86

I. Figures

Figure 1 Classification of haematological malignancies	9
Figure 2 Distribution of peripheral T- and NK-cell lymphoma	10
Figure 3 Representative histology of AITL infiltration in a lymph node	13
Figure 4 Schematic protein structure of <i>TET2</i>	18
Figure 5 Schematic protein structure of <i>DNMT3A</i>	20
Figure 6 Flowchart of final sample selection and study design	27
Figure 7 Representative AITL infiltration in bone marrow	38
Figure 8 Representative picture of DNA integrity analysis	39
Figure 9 Selection process of bone marrow samples for further molecular analysis.	40
Figure 10 NGS quality characteristics	42
Figure 11 Representative mutational findings analysed with the Integrative Variant Caller.....	45
Figure 12 Schematic protein structure of <i>TET2</i> including genetic variants of patients with AITL.....	49
Figure 13 Variant allelic frequencies in <i>TET2</i>	50
Figure 14 Schematic protein structure of <i>DNMT3A</i> including genetic variants of patients with AITL.....	51
Figure 15 Variant allelic frequencies in <i>DNMT3A</i>	52
Figure 16 Correlation of blood parameters with <i>TET2</i> mutation frequencies....	56
Figure 17 Comparison of blood parameters in subgroups with high and low <i>TET2</i> mutation frequencies	56
Figure 18 Divergent evolution of MDS and AITL in consequence of clonal haematopoiesis	68

II. Tables

Table 1 Recurrent genetic mutations in AITL	14
Table 2 AITL panel	30
Table 3 MDS panel.....	31
Table 4 Patient characteristics	36
Table 5 Bone marrow quality characteristics	41
Table 6 NGS quality characteristics	43
Table 7 Genetic profiles of subgroups.....	46
Table 8 Genetic variants	47
Table 9 Evaluation of germline variants	53
Table 10 Blood counts.....	55
Table 11 Genetic findings in MDS genes	58

III. Abbreviations

AITL	angioimmunoblastic T-cell lymphoma
AML	acute myeloid leukaemia
ASCT	autologous stem-cell transplantation
ASXL1	additional sex comb like 1 protein
BCL6	B-cell lymphoma 6 protein
bp	base pairs
CD	cluster of differentiation
CD10	cluster of differentiation 10, neprilysin
CDS	coding sequence
CHIP	clonal haematopoiesis of indeterminate potential
CXCL13	chemokine ligand 13, B-cell chemoattractant
Del	deletion
DNMT3A	DNA-methyltransferase 3 alpha
dNTP	deoxynucleoside triphosphate
EBV	Epstein-Barr virus
EDTA	ethylenediaminetetraacetic acid
Fe(II)	iron(II)
FFPE	formalin-fixed, paraffin-embedded
FLT3	Fms related receptor tyrosine kinase 3
FYN	protooncogene kinase FYN
GDP	guanosine diphosphate
GEF	guanine nucleotide exchange factor
GTP	guanosine triphosphate
Hb	haemoglobin
H&E	haematoxylin and eosin
ICOS	inducible T-cell costimulator

IDH1/2	isocitrate dehydrogenase 1/2
InDel	insertion-deletion
Ins	insertion
MDS	myelodysplastic syndrome
MgCl ₂	magnesium chloride
NADP ⁺	nicotinamide adenine dinucleotide phosphate
NGS	Next-generation sequencing
PD1	programmed cell death protein 1
PLC γ	phospholipase C γ
PTCL	peripheral T-cell lymphoma
PTCL-NOS	peripheral T-cell lymphoma, not otherwise specified
RAS	rat sarcoma protein, protooncogene
RHOA	ras homolog gene family, member A
rpm	rounds per minute
RUNX1	RUNX family transcription factor 1
SF3B1	splicing factor 3B subunit 1
SNP	single-nucleotide polymorphism
SRSF2	serine/arginine-rich splicing factor 2
TBE	Tris-Borate-EDTA
TCR	T-cell receptor
TET2	Tet methylcytosine dioxygenase 2
TFH	follicular T-helper cells
TP53	tumour suppressor protein 53
U2AF1	U2 small nuclear RNA auxiliary factor 1
VAF	variant allelic frequency
VAV1	vav guanine nucleotide exchange factor 1
ZRSR2	Zinc Finger CCCh-Type, RNA Binding Motif and Serine/Arginine rich 2

1 Introduction

1.1 The Impact and Systematic of lymphatic Malignancies

Haematological malignancies encompass a variety of tumours mutually deriving from neoplastic cells during haematopoiesis. The generation of blood cells is a multistep process, whereby malignant degeneration might occur on every stage leading to a wide range of manifestations with different clinical profiles. In general, three major groups of haematological malignancies can be discriminated in accordance with the developmental lineage: lymphomas, myelomas, and leukaemia. In dependence of the developmental level; however, malignancies differ tremendously in clinical appearance, therapy options and outcome. It is therefore of greatest importance to continuously classify subtypes in order to discover strategies to treat patients most reasonable (Arber et al., 2016, Swerdlow et al., 2017).

Amongst haematological malignancies, lymphomas represent neoplastic entities of lymphoid descent. Historically, they had been classified into Hodgkin and non-Hodgkin subtypes, which were first attempts to differentiate between patient subgroups under clinical and histopathological aspects (Stone, 2005). In the latest global cancer statistic of 2018, about 510.000 patients were estimated to get diagnosed and 250.000 patients to even die from one of non-Hodgkin lymphoma annually. Concerning Hodgkin lymphomas, numbers are lower but nonetheless decreasing. About 80.000 patients were estimated to be diagnosed and 26.000 to even die from this neoplastic disease annually (Bray et al., 2018). Although lymphomas are still commonly grouped into Hodgkin and non-Hodgkin, various subtypes could have been identified in the meantime. Greater emphasis is put on cellular lineage nowadays, due to further investigation on molecular and genetic characteristics, surface expression profiles and microscopical abnormalities. A consortium of different experts is continually revising and updating the classification system in accordance with current scientific knowledge. While classic Hodgkin lymphomas still constitute one group, numerous different non-Hodgkin lymphoma subgroups have been described and added mainly in the mature T- and NK-cell lymphomas (Swerdlow et al., 2017).

In the latest WHO classification from 2017, 18 heterogeneous subtypes of mature T- and NK-cell lymphomas have been described (**Figure 1**). A subgroup within mature T- and NK-cell lymphomas are peripheral T-cell lymphomas (PTCL), which derive from mature T-cells outside of the thymus, i.e. the angioimmunoblastic T-cell lymphoma. Taken together, PTCL are quite rare comprising only about 10 – 15% of all non-Hodgkin lymphomas (Vose et al., 2008). Nevertheless, mature T- and NK-cell lymphomas, especially PTCL, are of immense clinical significance due to common characteristics, including rapid progression, limited treatment options and finally poor therapeutic outcome. Overall, patients suffering from any subtype of PTCL have a 5-year overall survival of only 10 – 30% (Vose et al., 2008).

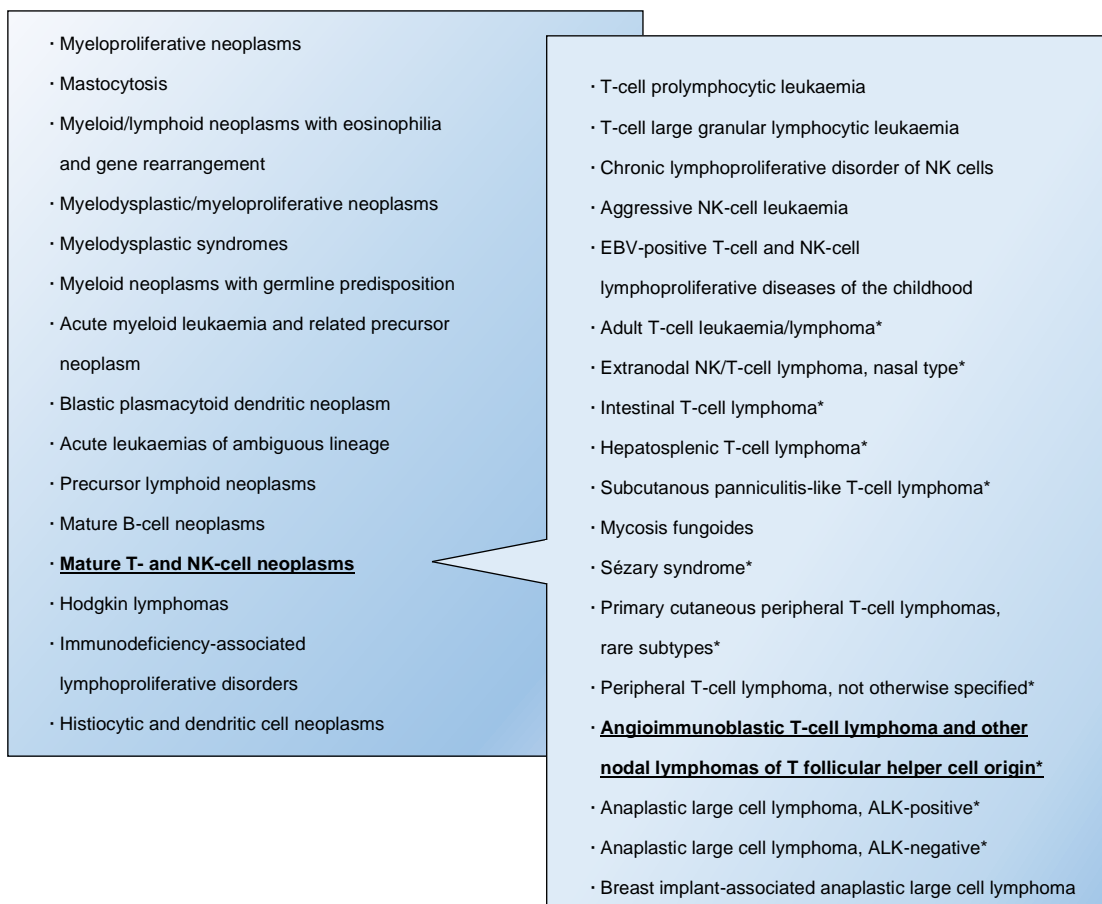


Figure 1 Classification of haematological malignancies. According to the latest WHO lymphoma consensus of 2017, 18 different subtypes of mature T- and NK-cell neoplasms can be distinguished (Swerdlow et al., 2017). Marked subtypes are also known as peripheral T-cell lymphoma (PTCL, *), including the angioimmunoblastic T-cell lymphoma (underlined).

1.2 Angioimmunoblastic T-Cell Lymphoma (AITL)

1.2.1 Epidemiology

Overall, approximately 15 – 30% of all PTCL and even 1 – 2% of all Non-Hodgkin lymphomas account for AITL (**Figure 2**). It is the second most common subtype of peripheral T- and NK-cell lymphomas after PTCL-NOS, although more recent studies suggest that it even might be the most frequent PTCL (de Leval et al., 2015). Annual incidences range between 0.1 – 0.2 per 100,000 in industrialized countries; however, numbers underlie geographic differences, as AITL seems to be more common in Europe compared with North America and Asia (Vose et al., 2008, de Leval et al., 2015). As an age-related malignancy, AITL mostly affects adults and elderly, the median age at onset ranges between 59 to 65 years. Concerning gender distribution, incidences of males and females are nearly equal (Dogan et al., 2017). Risk factors, including ethnicity or familiar predisposition in developing AITL were previously discussed, but still remain controversial (de Leval et al., 2010, Chihara et al., 2014). At least, various prognostic factors have been identified, which affect the clinical outcome. While extranodal involvement and increased age correlate with poor prognosis, elevated IgA levels and normal whole blood count have been identified as prognostically favourable factors (Tokunaga et al., 2012).

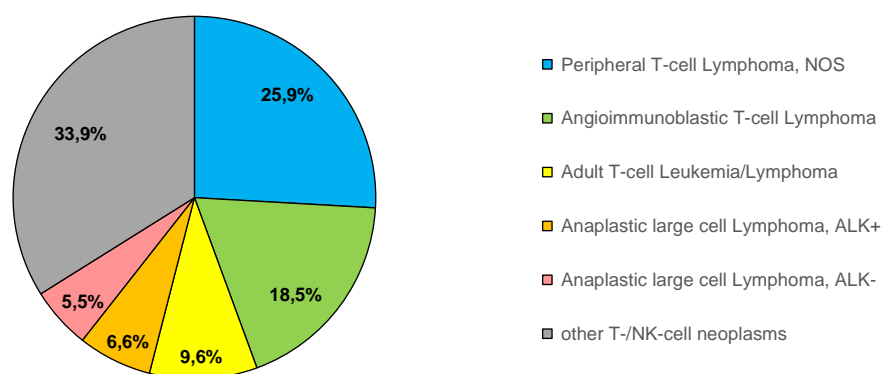


Figure 2 Distribution of peripheral T- and NK-cell lymphoma. In 2008, 1314 cases of peripheral T- and NK-cell lymphoma were distributed according to consensus diagnosis criteria. Therein, AITL represents the second most common subtype; however, incidences and distribution underlie geographic differences. The graph is modified from original (Vose et al., 2008).

1.2.2 Clinical Significance

First reports described AITL as *angioimmunoblastic lymphadenopathy with dysproteinaemia* relating to its clinical appearance (Frizzera et al., 1974). Generalized lymphadenopathy is the most common symptom, often accompanied by B symptoms (fever >38 °C, weight loss of >10% within 6 months, night sweats). Additional frequent clinical features are anaemia, thrombocytopenia, skin rashes, hepatosplenomegaly, hypergammaglobulinemia and systemic illness, which altogether reflect consequences of a dysregulated immune function (Federico et al., 2013). Bone marrow involvement is frequently reported, and seems to correlate with the extend of B symptoms and hepatosplenomegaly (Cho et al., 2009). In consequence to an ongoing dysregulation of the immune system, bacterial and fungal infections are associated and display the leading cause of death (de Leval et al., 2010).

Current therapy options are restricted, and the outcome is unfavourable. Multiple different agents and combinations have been tested so far; however, the best strategy to treat patients with AITL still remains unclear. While there is no targeted therapy available, anthracycline-based regimes such as CHOP (cyclophosphamide, doxorubicin, vincristine, prednisone) are mostly administered as first-line therapy showing median survival of about three years and 5-year overall survival rates of only 33% (Vose et al., 2008, Mourad et al., 2008). Apart from anthracycline-based regimes, additional agents have been tested, including immunomodulators (cyclosporine), monoclonal antibodies (Rituximab, Alemtuzumab, Zanolimab), histone deacetylase inhibitors (Belinostat) and proteasome inhibitors (Bortezomib), unfortunately without significant improvement. Most results are limited to phase II trials with response rates of only 30% or no significant increase in long-term survival (de Leval et al., 2010, Mosalpuria et al., 2014). Another promising approach relies on high-dose conditioning followed by autologous stem-cell transplantation (ASCT). Long-term survival rates of 56% after four years are even better than conventional chemotherapy; however, relapse rates of 51% after two years are reported. At least patients with an early stage of AITL seem to profit from an ASCT, which raises the need for diagnostic tools (Kyriakou et al., 2008).

1.2.3 Tumour Biology and Pathology

AITL displays a similar clinical presentation as other PTCL, commonly involving bone marrow, spleen, liver, and skin; however, lymph nodes are the prime organs of manifestation, which causes the leading symptom of generalized lymphadenopathy. In accordance with current expertise, mature follicular T-helper cells (TFH) are postulated as the normal counterpart of AITL, a subset of CD4⁺ lymphocytes, which are located inside germinal centres of lymph nodes (de Leval et al., 2007). The function within the lymphatic tissue relies on regulation of B-cell proliferation and initiation of an adaptive immune response. After encounter, B-cells undergo affinity maturation, class switch recombination and finally differentiation into plasma cells to sufficiently accomplish humoral conquer of antigens (Crotty, 2011). While this interaction is strictly controlled and the number of TFH is limited, neoplastic cells overcame this regulation. In AITL, the lymph node structure is destructed by ongoing proliferation and perinodal infiltration of small neoplastic lymphocytes, frequently accompanied by an increased number of follicular dendritic cells (**Figure 3**). The shape of lymphoma cells is distinct, only impaired by minor abnormalities, and clear cytoplasm administers a bright appearance. Clusters of tumour cells can often be spotted along high-endothelial venules (HEVs). In the inflammatory background, multiple cell types can be identified, amongst them histiocytes, eosinophils, and reactive lymphocytes. Interestingly, EBV-positive B-cells can be detected in 80-95% of all cases, probably due to reactive processes, which eventually might transform into B-cell lymphoma (Attygalle et al., 2007, Dogan et al., 2017).

In addition to microscopic features of AITL, surface expression profiles are fundamental for diagnostics. The immunophenotype of neoplastic AITL cells is characterized by pan-T-cell antigens, including similar expression patterns as normal TFH: CD4⁺, BCL6⁺, CD10⁺, CXCL13⁺, ICOS⁺, PD1⁺ (Dupuis et al., 2006, de Leval et al., 2007). Immunohistochemical staining of these antigens allows to distinguish between AITL and other PTCLs; however, none of the mentioned target molecules are AITL-specific. According to the WHO, the expression of at least two, better three of these markers is required for diagnosis (Swerdlow et al., 2017, Basha et al., 2019).

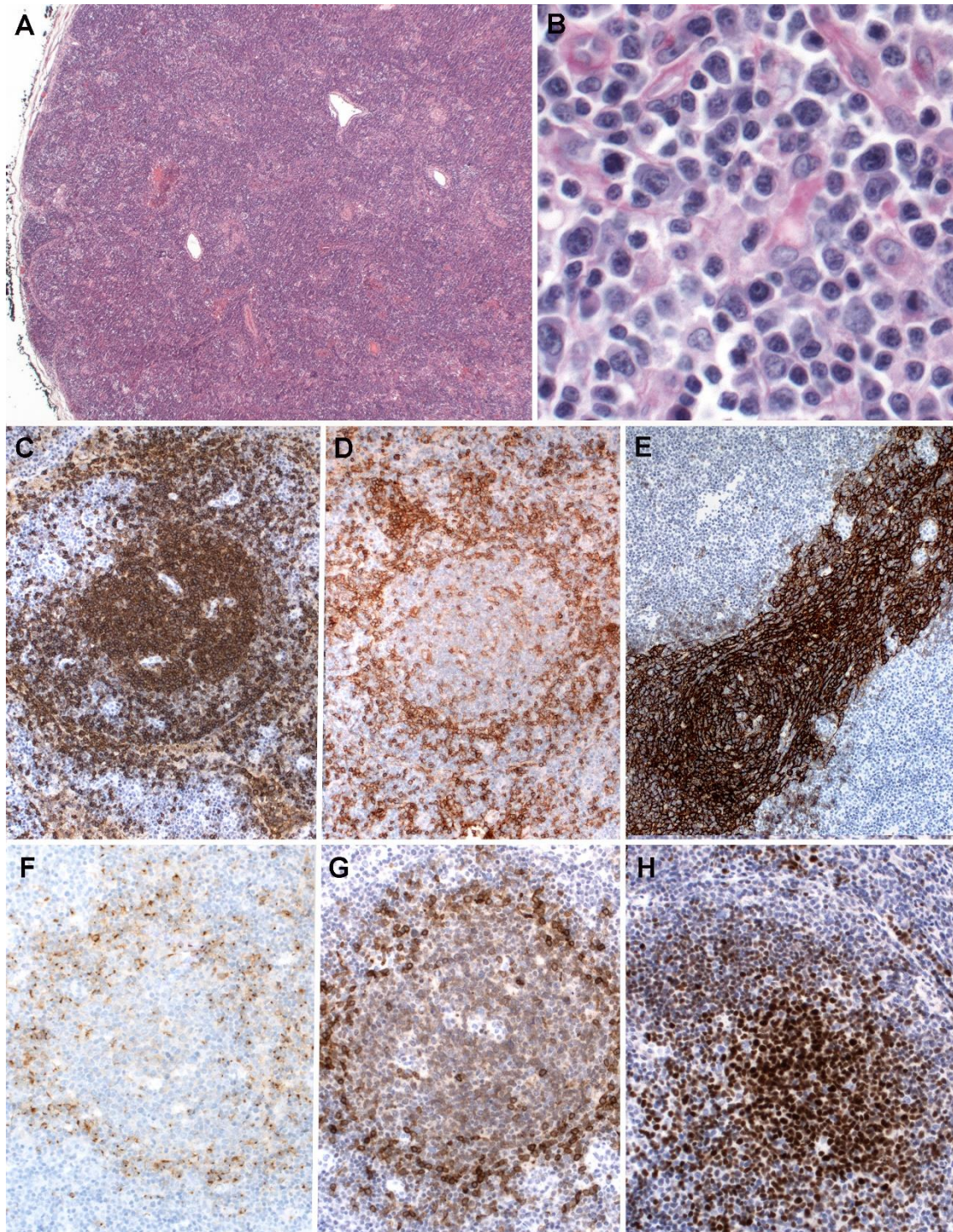


Figure 3 Representative histology of AITL infiltration in a lymph node. H&E stain shows the panoramic view of a lymph node with effacement of normal architecture and paracortical expansion with marked vascular proliferation (A, 5X). H&E stain reveals typical morphology of small to medium size neoplastic T-cells with clear to pale cytoplasm and irregular nuclei (B, 40X). Germinal centres are stained with CD20 (C, 10X) and CD4 stains neoplastic clear T-cells in the interfollicular area (D, 10X). The expanding follicular dendritic network is depicted by CD23 staining (E, 10X). neoplastic T-cells are positive for CXCL13 (F, 10X), CD10 (G, 20X) and BCL-6 (H, 20X). The pictures are kindly provided by the Institute of Pathology and Neuropathology at the University Hospital of Tübingen, Germany.

1.3 Genetic Profile of AITL

1.3.1 Frequent genetic Alterations

Since sequencing techniques have become standard tools in routine diagnostics, recurrent mutations have been found in AITL, predominantly involving pathways of signal transduction, epigenetics and T-cell receptor (TCR-) signaling (**Table 1**). The most frequently affected proteins represent the signal protein Ras homology family member A (RHOA), as well as the epigenetic regulators ten-eleven translocation methylcytosine dioxygenase 2 (TET2), isocitrate dehydrogenase 2 (IDH2) and DNA-methyltransferase 3 alpha (DNMT3A) (Fukumoto et al., 2018).

Table 1 Recurrent genetic mutations in AITL. The table is modified from original (Fukumoto et al., 2018).

	Frequencies (%)	References
Ras superfamily		
<i>RHOA</i>	50-70	(Sakata-Yanagimoto et al., 2014, Palomero et al., 2014, Yoo et al., 2014)
Epigenetic regulators		
<i>TET2</i>	47-83	(Lemonnier et al., 2012, Sakata-Yanagimoto et al., 2014)
<i>DNMT3A</i>	20-30	(Sakata-Yanagimoto et al., 2014, Palomero et al., 2014, Dobay et al., 2017)
<i>IDH2</i>	20-45	(Cairns et al., 2012, Sakata-Yanagimoto et al., 2014)
TCR signaling pathway		
<i>PLCγ</i>	14	(Vallois et al., 2016)
<i>CD28</i>	9-11	(Vallois et al., 2016, Rohr et al., 2016)
<i>FYN</i>	3-4	(Palomero et al., 2014, Vallois et al., 2016)
<i>VAV1</i>	5	(Vallois et al., 2016)

1.3.2 RHOA

RHOA is a small guanine nucleotide triphosphate (GTP)-binding protein belonging to a vast family of heterotrimeric signal transduction molecules. Hereby, RHOA acts as a molecular switch, alternating between an active, GTP-bound configuration and an inactive, dephosphorylated GDP-bound configuration. While GTP-bound, RHOA mediates several key processes, involving cell adhesion and migration, cell cycle regulation, as well as transcriptional control (Sakata-Yanagimoto et al., 2014). The switch into the active configuration is strictly regulated by the interaction with other molecules, for instance by guanine-exchange factor (GEF). This factor plays a crucial role, as its binding initiates the release of GDP and allows GTP binding (Palomero et al., 2014).

RHOA is encoded on chromosome 3 at position 21.31 and comprises 7 exons. The most prominent genetic alteration of *RHOA* constitutes a change of guanine to thymidine at position 50 in exon 2, which results in a switch of the 17th amino acid from glycine to valine. In AITL, *RHOA*^{G17V} is the most frequent genetic alteration, which is reported in 50 – 70% of all cases (Sakata-Yanagimoto et al., 2014, Yoo et al., 2014). While glycine is part of the GTP-binding site and crucial for activation, a substitution by valine impairs the exchange of GDP into GTP. The wildtype function in *RHOA*^{G17V} as a molecular switch is partially inhibited leading to a loss of function; however, the stimulation with GEF and other regulators remains unaffected (Sakata-Yanagimoto et al., 2014, Palomero et al., 2014). Besides functional loss, *RHOA*^{G17V} mutants show activation of different pathways compared to the wildtype, for instance stimulated TCR signalling via VAV1 binding. In addition to that, increased proliferation rates of mutated T-cell lines are observed. Taken together, *RHOA*^{G17V} highly supports the features of a driver mutation during AITL tumorigenesis due to its high frequencies and the downstream effects (Fujisawa et al., 2018).

Apart from AITL, altered *RHOA* is reported in patients with B-cell lymphomas underlining the impact of this gene on haematological malignancies. Studies showed mutation rates of about 6% in patients with Burkitt's lymphoma and of about 1% in diffuse large B-cell lymphoma (O'Hayre et al., 2016). Nevertheless,

mutation frequencies are strongly higher in malignancies of T-cell lineage, especially tumours with TFH phenotype. Within the subset of peripheral T-cell lymphomas, about 18% of patients with PTCL-NOS display *RHOA*^{G17V} (Kataoka and Ogawa, 2016). Furthermore, about 15% of patients with an adult T-cell leukaemia/lymphoma carry mutations within *RHOA*. Interestingly, *RHOA*^{C16R} was identified as the most frequent mutation, which affects the GTP-binding site at position 16 by an exchange of cysteine into arginine. In contrast to the loss-of-function mutation of *RHOA*^{G17V}, *RHOA*^{C16R} showed increased GTP/GDP cycling and enhanced downstream transcription activity (Nagata et al., 2016). Taken together, RHOA plays a crucial role in haematopoietic balance, as mutations are well described pushing tumorigenesis into various B- and T-cell neoplasms.

1.3.3 IDH2

IDH2 is a NADP⁺-dependent isocitrate dehydrogenase catalysing the oxidative decarboxylation of isocitrate to α -ketoglutarate. As a key enzyme of citric acid, it is involved in the mitochondrial metabolism and energy production. Moreover, isocitrate dehydrogenases contribute to epigenetic regulation. Analysis on patients with mutated *IDH2* showed extended hypermethylation patterns, especially in promotor areas causing aberrant transcriptional profiles (Figueroa et al., 2010).

IDH2 comprises 12 exons and is encoded on chromosome 15 at position 26.1. Genetic alterations are found in several neoplastic entities, amongst them haematopoietic malignancies. In patients with AITL, mutation frequencies of 20 – 45% are reported, most prominently at the active site of an arginine residue at position 172 (Sakata-Yanagimoto et al., 2014, Cairns et al., 2012). Aberrant *IDH2*^{R172} leads to an increased production and accumulation of the oncometabolite D-2-hydroxyglutarate, which affects different aspects of tumorigenesis, involving histone and DNA methylation, angiogenesis and metabolic dysregulation (Cairns et al., 2012, Fukumoto et al., 2018). In addition to AITL, about 12% of all AML patients display mutated *IDH2*; however, at a

different position. *IDH2^{R140}* is specific to AML leading to impaired haematopoietic differentiation and gene expression profiles of stem and progenitor cells. Interestingly, IDH2 represents a therapeutic target structure. Since 2017, relapsed or refractory AML can specifically be treated with Enasidenib, a small molecule inhibitor against IDH2 (Figueroa et al., 2010, Stein et al., 2017).

Apart from blood cancer, enhanced levels of D-2-hydroxyglutarate can also induce hydroxyglutaric aciduria and subsequently damage the brain, for instance evoke seizures or impair important functions as vision, speech, and memory. Moreover, Mutations are strongly correlated with gliomagenesis. *IDH2^{R172}* and *IDH1^{R132}* had been identified to progress tumorigenesis of various malignant gliomas, as these mutations have a high clinical and prognostic significance; however, mutation frequencies of *IDH2* are only around 3% in all glial tumours (Yan et al., 2009, Cohen et al., 2013). Overall, *IDH2^{R172}* is not exclusive to haematopoietic malignancies, but very specific to AITL and undoubtedly associated with malignant transformation.

1.3.4 TET2

TET2 comprises 11 exons and is encoded on chromosome 4 at position 24. As an epigenetic regulator, its key function relies on transcriptional control by converting 5-methylcytosine into 5-hydroxymethylcytosine. The catalytic domain is preserved on the double-stranded β helix dioxygenase domain at the carboxyl-terminal end of the protein (**Figure 4**). This domain harbors two α -ketoglutarate- and Fe(II)-binding sites, which are necessary for the oxidation activity. Moreover, *TET2* comprises a cysteine-rich domain in the middle of the protein (Hu et al., 2013, Nakajima and Kunimoto, 2014). Crystal structure analysis suggested the protein to form a complex entity during catalysis and DNA interaction. The cysteine-rich domain hereby seems to stabilize its integrity, which is necessary for substrate recognition (Hu et al., 2013).

TET2 is widely expressed; however, its role in molecular processes is not fully understood. Mutations are found in patients with various myeloid abnormalities, suggesting a central function in the development of blood cells, stem cell function and cellular transformation (Figuroa et al., 2010, Moran-Crusio et al., 2011). Loss-of-function mutations are associated with myelodysplastic syndromes (MDS), myeloproliferative disorders, and AML. Overall, about 10 – 20% of all myeloid cancers carry somatic alterations in *TET2* (Delhommeau et al., 2009, Langemeijer et al., 2009). Apart from myeloid malignancies, genetic alteration of *TET2* is also found in T-cell lymphoma; however, almost exclusively in AITL and PTCL-NOS with TFH phenotype. Besides *RHOA*, *TET2* is the most frequently altered gene in patients with AITL, as mutations are found in even 47 – 83%. Interestingly, about two-thirds of patients with genetically altered *TET2* harbour even two or three different mutations (Lemonnier et al., 2012, Sakata-Yanagimoto et al., 2014). Although mutations are seen in most of the patients, its role during tumorigenesis seems unclear. Altered *TET2* is reported to accumulate over time and are even found in healthy elderly exceeding incidences of diagnosed haematopoietic malignancies suggesting clonal haematopoiesis of indeterminate potential (CHIP, see below) (Jaiswal et al., 2014).

Interestingly, *TET2* and *IDH2* mutations co-occur in patients with AML, suggesting *TET2* to be a main target of IDH2-mediated oncometabolites. Abnormal D-2-hydroxyglutarate accumulates in individuals with aberrant IDH2 function and seems to impair the catalytic activity of *TET2* (Figuroa et al., 2010). Similar interactions exist in AITL, as *IDH2*^{R172} and *RHOA*^{G17V} are almost always found in patients with mutated *TET2* (Steinhilber et al., 2019).

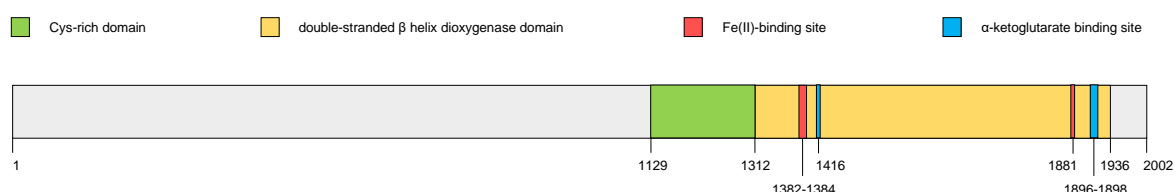


Figure 4 Schematic protein structure of TET2. The catalytic activity of TET2 relies on the double-stranded β helix dioxygenase domain at the carboxyl-terminal end of the protein. Within this domain, two distinct Fe(II)- and α-ketoglutarate binding-sites are necessary for catalytic activity. In the middle of the protein, a cysteine-rich domain is located, which is supposed to stabilize the complex entity and enables substrate recognition. The graphic was modified from original (Hu et al., 2013).

1.3.5 DNMT3A

DNMT3A is located on chromosome 2 at position 23.3 and encoded by 23 exons. It belongs to a family of DNA methyltransferases, which play a crucial role in epigenetic regulation of gene expression. The protein structure of DNMT3A is characterized by a proline- and tryptophan-rich (PWWP-) domain, the Zinc-finger ATRX-DNMT3-DNMT3L (ADD-) domain and the catalytic domain at the carboxy-terminal end (**Figure 5**). At the catalytic site, the enzyme attaches methyl groups to the pyrimidine ring of cytosines, especially on CpG dinucleotides located upstream in promotor areas. PWWP- and ADD-domains are less well understood, but seem to be associated with protein-interaction and histone-linking (You and Jones, 2012, Yang et al., 2015).

DNMT3A is involved in a variety of different developmental processes, amongst them embryonic and haematopoietic stem cell differentiation. Especially the association of mutant variants with blood cancer highlights the potential to drive malignant transformation (Yang et al., 2015). In murine models, loss of function contributes to a clonal expansion and haematopoietic abnormalities. Most interestingly, the absence of DNMT3A leads to hyper- and hypomethylation at distinct loci. For instance, CpG islands of tumour suppressor genes show higher levels of hypermethylation and therefore reduced activity. Whereas hypomethylation, and subsequently incomplete repression of the gene, seems to occur in stem cell specific genes (Challen et al., 2011).

Analysis on patients with AML showed mutations in *DNMT3A* of about 22% (Ley et al., 2010). Interestingly, mutation frequencies are higher than other genetic findings, which suggest *DNMT3A* as an early event with clonal expansion. About 60% of *DNMT3A*-mutant patients harbour a mutation within the catalytic domain at the arginine residue at position 882, which reveals an inhibited wildtype activity (Yang et al., 2015). In AITL, about 20 – 30% of the patients display mutations within *DNMT3A*; however, there is a strong association with other genetic targets. For instance, 70 – 100% of *DNMT3A*-mutated patients also display genetic variations in *TET2* (Sakata-Yanagimoto et al., 2014, Yang et al., 2015).

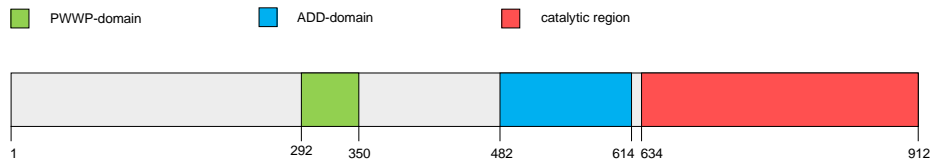


Figure 5 Schematic protein structure of DNMT3A. Three different protein domains can be distinguished, including a proline- and tryptophan-rich (PWWP-) domain, the Zinc-finger ATRX-DNMT3-DNMT3L (ADD-) domain and the catalytic region at the carboxy-terminal end of the protein. While PWWP- and ADD-domains are necessary for interaction with histones and other proteins, the catalytic domain enables attachment of methyl-groups during epigenetic processes. The graphic was modified from original (Couronne et al., 2012, Yang et al., 2015).

1.4 Clonal Haematopoiesis of indeterminate Potential

Clonal haematopoiesis of indeterminate potential (CHIP) is defined as a subset of cells, which clonally expand due to genetic alterations, but do not necessarily lead to malignant transformation. Somatic mutations of these genes are commonly at a VAF of at least 2% and associated with haematological neoplasms, i.e. *DNMT3A*, *TET2*, *TP53*, *ASXL1*, *SRSF2*, etc. (Steensma et al., 2015). Since NGS has become an affordable tool in medical research, further insights into mutational dynamics during malignant bone marrow transformation were gained. While haematopoiesis is strictly controlled, cells within bone marrow might acquire somatic mutations and begin to transform. These CHIP cells might evolve into an MDS, a well-described preleukaemic disease and clonal disorder of hematopoietic cells causing immature red blood cells, white blood cells and platelets. More than 50 different genes are described to be mutated in MDS, amongst them *TET2* and *DNMT3A*, which are most frequently found and seem to occur at an early stage (Papaemmanuil et al., 2013, Sperling et al., 2017). Unfortunately, about a third of patients with MDS progress into AML, and therefore, show an aggravated clinical situation. Morbidity and Mortality in patients with MDS are mainly consequence of the pancytopenia and secondary AML (Ades et al., 2014).

While MDS describes a preleukaemic bone marrow failure syndrome, genetic alterations might also lead to clonal expansion without haematological deficits. CHIP mutations seem to play an initiating role in AITL. Different groups have already reported higher variant allelic frequencies (VAF) in *TET2* and *DNMT3A* compared with *RHOA*^{G17V} or *IDH2*^{R172} in AITL, which suggest them as earlier events during tumorigenesis (Quivoron et al., 2011, Couronne et al., 2012). Recent studies confirm this hypothesis and emphasise the impact of *TET2* during tumorigenesis. Patients with an *IDH2*^{R172} and/or *RHOA*^{G17V} mutations almost always revealed altered *TET2*, whereas *DNMT3A* was only mutated in about half of these cases. Patients without *IDH2*^{R172} or *RHOA*^{G17V} displayed similar mutation rates for both, *TET2* and *DNMT3A*, in about half of the cases, suggesting both genes as CHIP mutations with a major impact of *TET2* and raised the rationale for further investigations (Steinhilber et al., 2019).

1.5 Aim of the Thesis

AITL harbours a characteristic mutational landscape, amongst its variations of *RHOA*, *IDH2*, *DNMT3A* and *TET2*. While *RHOA*^{G17V} and *IDH2*^{R172} represent specific mutations, which are almost exclusively found in patients with AITL, the roles of genetically altered *DNMT3A* and *TET2* during tumorigenesis still remain unclear. Mutations within these two epigenetic regulators are diverse, less specific to AITL and even accumulate in healthy individuals throughout life (Jaiswal et al., 2014). The high allelic frequency in AITL and the strong association with multiple haematological cancers; however, strongly indicates that *DNMT3A* and *TET2* are associated with tumorigenesis of AITL. Moreover, recent studies suggest these two genes to be involved in CHIP (Lewis et al., 2020). Therefore, it is of greatest interest to examine the mutational dynamics between the different genes and subsequently elucidate the impact on *RHOA* and *IDH2* mutations.

In this study, the role of *TET2* and *DNMT3A* will be addressed by comparison of their genetic profile in haematopoietic progenitors to unveil their role in AITL. If mutations within these genes contribute as CHIP mutations to tumorigenesis, clonal expansion of a cellular subset will occur prior to mutational findings in *RHOA*^{G17V} or *IDH2*^{R172}. Hereby, bone marrow samples around the diagnosis of AITL will be compared with AITL infiltrated lymph node biopsies to determine the presence and VAF of *RHOA*, *IDH2*, *DNMT3A* and *TET2* mutations. Mutations of the four genes will be detected in bone marrow samples of patients with diagnosed AITL using NGS and matched with their genetic profile of lymph nodes. Bone marrow not only represents the physiological habitat of haematopoietic progenitors, but samples are also commonly gained during clinical routine diagnostic and therefore accessible.

2 Material and Methods

2.1 Materials

2.1.1 Patient samples

Formalin-fixed, paraffin-embedded (FFPE) bone marrow samples of 22 patients with diagnosed AITL in lymph nodes were retrieved from the files of the Institute of Pathology and Neuropathology at the University Hospital of Tübingen. The cases included were part of a previous study, where a complete genetic analysis was performed in 50 cases of AITL in lymph nodes (Steinhilber et al., 2019). Due to the presence of up to three bone marrow samples per patient, a total of 30 bone marrow samples dating back from 2005 to 2017 were included into this study. Slides at a thickness of 2.5 µm were cut by experienced technicians for subsequent use, involving H&E staining and DNA extraction. Only cases with known mutations concerning *RHOA*, *IDH2*, *DNMT3A* and *TET2* were included, if a corresponding bone marrow biopsy was performed by staging purposes at the moment of the diagnosis. If data was missing, FFPE lymph nodes were retrieved and processed similar to the previous study. Written consent was obtained for this study by the local ethics committee of the University (090/2016BO2).

2.1.2 Chemicals and Reagents

<i>Chemicals and Reagents</i>	<i>Company</i>
Agencourt AMPure XP	Beckman Coulter
dNTP	Thermo Fisher Scientific
Ethanol absolute	AppliChem
GelRed® Nucleic Acid Gel Stain	Biotium
GeneRuler 100 bp DNA Ladder	Thermo Fisher Scientific
Invitrogen™ UltraPure™ Distilled Water	Thermo Scientific
LE Agarose	Biozym
TBE Buffer (10X, 1 L):	
890 mM Tris	Sigma-Aldrich
890 mM Boric acid	Merck
25 mM EDTA	AppliChem
TriTrack DNA Loading Dye	Thermo Fisher Scientific

2.1.3 Kits

<i>Kit</i>	<i>Company</i>
AmpliTaq Gold® DNA Polymerase	Thermo Fisher Scientific
Ion 510™ & Ion 520™ & Ion 530™ Kit – Chef	Thermo Fisher Scientific
Ion 520™ Chip – Kit	Thermo Fisher Scientific
Ion AmpliSeq™ Library Kit 2.0 - 96LV	Thermo Fisher Scientific
Ion Library TaqMan™ Quantitation Kit	Thermo Fisher Scientific
NEBNext® FFPE DNA Repair Mix	New England Biolabs
Maxwell® RSC FFPE Plus DNA Purification KIT	Promega Corporation
Qubit™ dsDNA HS Assay Kit	Thermo Fisher Scientific

2.1.4 Consumable supplies

Consumable supplies for daily laboratory routine, involving reaction tubes, pipette tips, medical examination gloves, et cetera were obtained from the following companies: Abena, Biozym, Eppendorf, Falcon, Greiner, Neolab and Sarstedt.

2.1.5 Oligonucleotide Sequences

PCR Primer to assess DNA integrity

<i>Primer</i>	<i>Sequence (5′ - 3′ orientation)</i>
AF4/X3U	GGAGCAGCATTCCATCCAGC
AF4/X3L	CATCCATGGGCCGGACATAA
AF4/X11U	CCGCAGCAAGCAACGAACC
AF4/X11L	GCTTTCCTCTGGCGGCTCC
PLZF/X1U	TGCGATGTGGTCATCATGGTG
PLZF/X1L	CGTGTCATTGTCTGTGAGGC
RAG1/X2U	TGTTGACTCGATCCACCCCA
RAG1/X2L	TGAGCTGCAAGTTTGGCTGAA
TBXAS1/X9U	GCCCGACATTCTGCAAGTCC
TBXAS1/X9L	GGTGTGGCCGGGAAGGGTT

Ion Xpress™ Barcoding Adapters (example)

<i>Barcode</i>	<i>Sequence (5′ - 3′ orientation)</i>
IonXpress_007	TTCGTGATTC

2.1.6 Devices

<i>Utilization</i>	<i>Device</i>	<i>Company</i>
Centrifuge	Combi-Spin FVL-2400N	Peqlab
	Heraeus Multifuge 1L-R	Thermo Fisher Scientific
	PerfectSpin Mini centrifuge	Peqlab
DNA Extraction	Maxwell® RSC Instrument	Promega Corporation
Fluorometer	Qubit® Fluorometer	Thermo Fisher Scientific
Gel Electrophoresis	PerfectBlue™ Minigelsystem	Peqlab
	LKB GPS 200/400	Pharmacia
Gel Imaging	Quantum Gel Documentation System	Peqlab
NGS system	Ion Torrent Ion Chef™ System	Thermo Fisher Scientific
	Ion Torrent Ion S5™ System	Thermo Fisher Scientific
Microscope	Axiostar 2	Carl Zeiss
Pipettes	PIPETMAN® Classic	Gilson
	Research® plus	Eppendorf
Spectrophotometer	NanoDrop™ 2000	Thermo Fisher Scientific
Thermal Cyclers	GeneTouch Thermal Cycler	Biozym
	Mastercycler® nexus X2/GX2e	Eppendorf
	LightCycler® 480 II	Roche
Thermoshaker	Thriller®	Peqlab
Vortexer	Vortex-Genie™ 2	Scientific Industries SI™
Workstations	HERAsafe™ biological safety cabinet	Thermo Fisher Scientific
	UV Sterilizing PCR workstation	Peqlab

2.1.7 Software

<i>Utilization</i>	<i>Software</i>	<i>Company</i>
Citation/Reference management	EndNote™ X9.1	Clarivate Analytics
Gel Imaging	BioCapt (v. 11.03)	Vilber Lourmat
	Integrative Genomics Viewer (v. 2.3)	Broad Institute
Graphic Design	GraphPad Prism (v. 5.00)	GraphPad Software
Patient/Sample management	PAS NET	Nexus
Primer Design	Primer3 (v. 0.4.0)	Whitehead Institute for Biomedical Research
Raw data analysis	Ion Torrent Suite Software 5.4	Thermo Fisher Scientific
Variant caller	Ion Torrent Variant Caller 5.4	Thermo Fisher Scientific
Writing	Word 2016	Microsoft

2.1.8 Companies

<i>Company</i>	<i>Headquarter</i>
Abena	Aabenraa, Denmark
AppliChem	Darmstadt, Germany
Beckman Coulter	Brea, CA, United States of America
Biotium	Fremont, CA, United States of America
Biozym	Oldendorf, Germany
Carl Zeiss	Oberkochen, Germany
Clarivate Analytics	Philadelphia, PA, United States of America
Eppendorf	Hamburg, Germany
Falcon	Corning, NY, United States of America
Gilson	Middleton, WI, United States of America
GraphPad Software	La Jolla, CA, United States of America
Greiner	Kremsmünster, Austria
Merck	Darmstadt, Germany
Microsoft	Redmond, WA, United States of America
Neolab	Heidelberg, Germany
New England Biolabs	Ipswich, MA, United States of America
Nexus	Villingen-Schwenningen, Germany
Peqlab	Erlangen, Germany
Pharmacia	Uppsala, Sweden
Promega Corporation	Fitchburg, WI, United States of America
Roche	Basel, Switzerland
Sarstedt	Nümbrecht, Germany
Scientific Industries SI™	Bohemia, NY, United States of America
Sigma-Aldrich	St. Louis, MO, United States of America
Thermo Fisher Scientific	Waltham, MA, United States of America
Vilber Lourmat	Eberhardzell, Germany

2.2 Study Design

Bone marrow samples of patients with AITL were selected and evaluated prior to sequencing experiments (**Figure 6**).

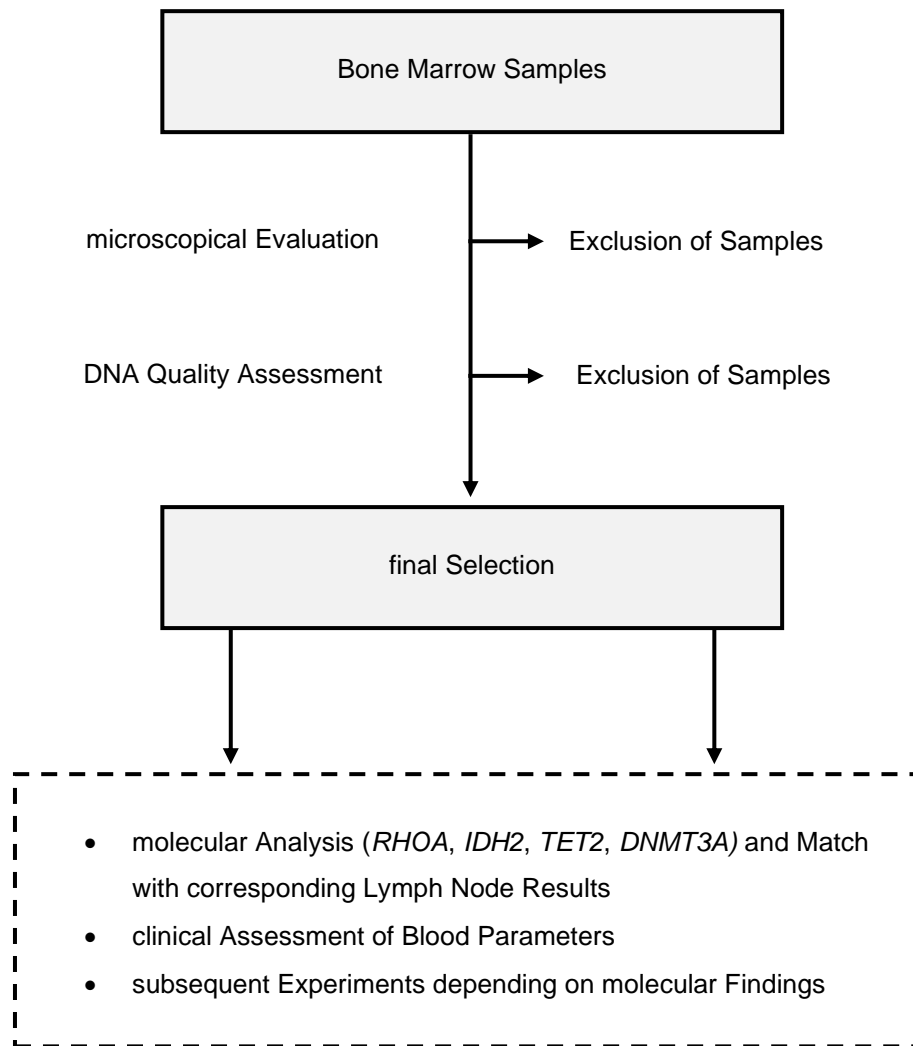


Figure 6 Flowchart of final sample selection and study design. After an initial selection of appropriate cases, bone marrow samples were evaluated in terms of quality prior to further analysis. Hereby, two aspects were considered, microscopical assessment and evaluation of DNA integrity.

2.3 Microscopy

All available slides from routine diagnostics, including immunohistochemistry, of all bone marrow biopsies were evaluated together with Prof. Dr. Leticia Quintanilla-Fend microscopically. Only samples were approved for subsequent use, if a microscopical evaluation was feasible. Bone marrow specimens were excluded from further studies, if cell numbers were too low or the tissue itself was of poor quality under histopathologic aspects. In addition, microscopy was also conducted to estimate the proportion of hematopoietic cells and to detect possible lymphoma infiltration. Microscopical pictures were taken together with Ivonne Montes and kindly provided by the Institute of Pathology and Neuropathology at the University Hospital of Tübingen, Germany.

2.4 DNA Extraction

Rolls of FFPE bone marrow slices were stored in 1.5 mL reaction tubes at room temperature until DNA extraction with the Maxwell® RSC FFPE Plus DNA Purification KIT. Samples were initially incubated at 70 °C and 400 rpm in a thermoshaker for about 5 min until complete dewaxing. Proteolysis was conducted afterwards by adding 25 µL proteinase K and 225 µL proteolysis buffer to each sample, followed by additional incubation at 70 °C and 400 rpm in a thermoshaker for 6 – 12 hours. DNA was purified afterwards according to the protocol of the manufacturer using the Maxwell® RSC device and reagents and finally eluted in 60 µL nuclease-free water. After quantitation of DNA yield with NanoDrop™ 2000 Spectrometer, extracts were stored at -20 °C.

2.5 DNA Quality Assessment

2.5.1 Polymerase Chain Reaction

Besides spectrophotometric evaluation of isolated DNA, samples were amplified by polymerase-chain reaction (PCR) in order to assess DNA integrity using the AmpliTaq Gold® DNA Polymerase Kit by Thermo Fisher Scientific. All steps were conducted according to the manufacturer. PCR experiments were set up in a total

volume of 25 μL , including 2.5 μL of 10X PCR Gold Buffer, 1.5 mM MgCl_2 , 0.2 mM dNTP mix, 0.2 μM forward and reverse primer, 1.25 U AmpliTaq Gold® DNA Polymerase, 10 – 50 ng template DNA and filled up with DNase- and RNase-free and UV-treated water. Samples with water instead of DNA were included into experimental setup and considered as negative controls. In the following, reaction mixtures were incubated in a thermal cycler, a detailed program is shown below, analysed via gel electrophoresis, and stored at $-20\text{ }^\circ\text{C}$.

Thermal Cycler Program

Initial Denaturation	95 $^\circ\text{C}$		7 min	
Denaturation	95 $^\circ\text{C}$	45 s	} 35 cycles	
Annealing	60 $^\circ\text{C}$	45 s		
Extension	72 $^\circ\text{C}$	60 s		
Final extension	72 $^\circ\text{C}$		4 min	
Hold	16 $^\circ\text{C}$		forever	

2.5.2 Gel Electrophoresis

Gel electrophoresis was used to separate PCR products to evaluate the integrity of each DNA sample. Initially, 2% agarose gels were moulded containing 2 g agarose dissolved in 100 mL TBE buffer. TBE buffer also served as loading buffer during electrophoresis. GelRed® Nucleic Acid Gel Stain was added to gels before consolidation as intercalating reagent for UV detection of amplified DNA. After consolidation, 10 μL of PCR products were mixed with 2 μL 6X TriTrack DNA Loading Dye and gently transferred into gel pockets. In order to determine the size of amplified products, a DNA ladder composed of different fragments varying from 100 – 1000 bp was added to the gel. Therefore, 1 μL of the loading dye was mixed with 4 μL deionised water and 1 μL GeneRuler 100 bp DNA Ladder and included in each run. After about 20 min at 180 V, gels were transferred into Quantum Gel Documentation System by Peqlab and illuminated with UV. BioCapt software was used to visualise, print, and save results.

2.5.3 DNA Repair

DNA samples showing an integrity of 200 bp or less were treated with the NEBNext® FFPE DNA Repair Mix before sequencing experiments. 200 ng DNA in a total volume of 53.5 µL was mixed with 6.5 µL Repair Buffer and 2 µL Mix and incubated at room temperature for 15 min. Afterwards, DNA was purified with AMPure XP magnetic beads according to the manufacturer. Successful DNA repair was subsequently confirmed with repeated PCR to analyse DNA integrity.

2.6 Ion Torrent™ Next-Generation Sequencing

2.6.1 AITL Panel

NGS was conducted on all cases using an Ion AmpliSeq Custom panel by Thermo Fisher Scientific, which was designed using the Ion AmpliSeq Designer (version 6.0.4). A table of all genes, which are covered by this panel, is shown below (**Table 2**).

Table 2 AITL panel. An AmpliSeq custom panel for the analysis of AITL.

Gene	Transcript	Position (GRCH37/hg19)	Exon(s)	Amplicons	Coverage of CDS %
<i>DNMT3A</i>	NM_022552	chr2: 25,457,148 – 25,536,853	CDS	47	95.75
<i>IDH2</i>	NM_002168	chr15: 90,631,814 – 90,631,957	4	2	-
<i>RHOA</i>	NM_001664	chr3: 49,412,916 – 49,413,022	2	1	-
<i>TET2</i>	NM_001127208	chr4: 106,155,100 – 106,197,676	CDS	68	98.51

coding sequence (CDS)

2.6.2 MDS Panel

NGS was conducted on a subset of cases using an Ion AmpliSeq Custom panel by Thermo Fisher Scientific, which was designed using the Ion AmpliSeq Designer (version 6.0.4). A table of all genes, which are covered by this panel, is shown below (**Table 3**).

Table 3 MDS panel. An AmpliSeq custom panel for the analysis of MDS.

Gene	Transcript	Position (GRCH37/hg19)	Exon(s)	Amplicons	Coverage of CDS %
ASXL1	NM_015338	chr20: 31,021,082 – 31,021,725	11	7	-
		chr20: 31,022,230 – 31,024,815	12	27	-
		chr20: 31,024,841 – 31,025,141	12	4	-
CBL	NM_005188	chr11: 119,148,462 – 119,149,428	7-9	6	-
DNMT3A	NM_022552	chr2: 25,468,890– 25,471,126	7-12	12	-
		chr2: 25,457,148– 25,468,206	13-23	23	-
FLT3	NM_004119	chr13: 28,608,214 – 28,608,351	14	2	-
		chr13: 28,592,608 – 28,592,712	20	1	-
IDH1	NM_005896	chr2: 209,113,088 – 209,113, 194	4	1	-
IDH2	NM_002168	chr15: 90,631, 814– 90,631,955	4	2	-
KRAS	NM_033360	chr12: 25,398,203 – 25,398, 310	2	1	-
		chr12: 25,380,260 – 25,380, 337	3	1	-
		chr12: 25,378,543 – 25,378,663	4	2	-
NRAS	NM_002524	chr1: 115,258,687 – 115,258,781	2	1	-
		chr1: 115,256,463 – 115,256,578	3	1	-
		chr1: 115,252,185 – 115,252,309	4	1	-
RUNX1	NM_001754	chr21: 36,164,432 – 36,421,196	CDS	20	89.23
SETBP1	NM_015559	chr18: 42,531,789 – 42,531, 951	4	2	-
SF3B1	NM_012433	chr2: 198,266,704 – 198,267,554	14,15	6	-
SRSF2	NM_003016	chr17: 74,732,889 – 74,733,028	1	1	-
TP53	NM_000546	chr17: 7,572,927– 7,579,912	CDS	22	97.69
U2AF1	NM_006758	chr21: 44,524,432 – 44,524,508	2	1	-
		chr21: 44,514,760 – 44,514,832	6	1	-
ZRSR2	NM_005089	chrX: 15,808,619 – 15,841,365	CDS	22	92.56

coding sequence (CDS)

2.6.3 Generation of Amplicon Libraries

Amplicon libraries were generated for NGS with the Ion AmpliSeq™ Library Kit 2.0 - 96LV. All steps and reagents were conducted according to the manufacturer. Initially, a PCR experiment was conducted in a total volume of 20 µL per sample, including 4 µL of 5X Ion AmpliSeq™ HiFi Mix, 10 µL of AITL primer pool 1 or 2 of the custom panel, 10 ng of double-stranded template DNA in a volume of maximum 6 µL and filled up with UV-treated deionised water. The concentration of double-stranded DNA in each sample was assessed in advance with the Qubit™ dsDNA HS Assay Kit and the Qubit® Fluorometer. PCR mixes were incubated in a thermal cycler, the program is shown below. After an initial amplification of template DNA, remaining oligonucleotide primers were partially digested by adding 2 µL FuPa reagent to each sample with subsequent incubation. In the following, ligation with barcoding sequencing adaptors was conducted. Therefore 2 µL of Ion Xpress™ Barcoding Adapters were added to each sample and incubated. Finally, amplicon libraries were purified with AMPure XP magnetic beads according to the manufacturer. Incubation protocols are shown below:

Thermal Cycler Program: Amplicon Generation

Initial Denaturation	99 °C	2 min		
Denaturation	99 °C	15 s	} 24 cycles	
Annealing/Extension	60 °C	4 min		
Final extension	72 °C	4 min		
Hold	16 °C	forever		

Oligonucleotide Primer Digestion

50 °C	10 min
55 °C	10 min
60 °C	10 min

Barcode Adapter Ligation

22 °C	30 min
72 °C	10 min
10 °C	up to 1 h

2.6.4 Quantification of Amplicon Libraries

After generation and purification of libraries, amplicons were quantified via real-time PCR with the Ion Library TaqMan™ Quantitation Kit. Therefore, libraries were diluted 1:500 by adding 2 µL of DNA product to 998 µL deionised water, followed by brief vortexing. Hereafter, 4.5 µL diluted library was mixed with 5 µL Ion Library Taqman® qPCR Mix and 0.5 µL Ion Library Taqman® Quantitation Assay and transferred into a 96-well light cycler plate. All experiments were conducted in duplicates, samples with water instead of DNA were included into experimental setup and considered as negative controls. In addition, three defined standard concentrations of modified *Escherichia coli* DH10B control library were added to each experiment for subsequent calculation. The thermal cycler program is shown below:

Real-Time PCR Program: Library Quantification

50 °C	2 min	} 40 cycles
95 °C	3 s	
60 °C	30 s	

2.6.5 Chip Loading and Sequencing

Clonal amplification, enrichment and chip loading were done with the Ion Torrent Ion Chef™ and sequencing was conducted using the Ion S5™ System by Thermo Fisher Scientific and the support of experienced technicians. Amplicon library pools were initially diluted to a concentration of 100 pM with DNase- and RNase-free and UV-treated water. Twelve libraries for AITL, or eight libraries for MDS were then pooled and diluted to a concentration of 27.5 pM and finally transferred into the cartridge of the Ion Chef™ System. In the following the automated system conducted annealing of amplicon to Ion Sphere™ Particles of the Ion 510™ & Ion 520™ & Ion 530™ Kit – Chef, as well as enrichment and loading. After 13 – 18 h run time, products were transferred into the Ion S5™ System on an Ion 520™ chip and run for another 2 – 3 h. In the following, raw data was uploaded on the Ion Torrent server for analysis.

2.6.6 Genetic Analysis

Genetic analysis on raw data was accomplished with Ion Torrent Suite Software (Version 5.4). The implemented Torrent mapping alignment program was used to align reads to the human reference sequence build 38 (hg19). With the Ion Reporter Software, data was then analysed concerning genetic alterations. The detection threshold for variants was set at an allelic frequency of 1%. Each mutation was visualised with the Integrative Genomics Viewer to exclude artefacts and reviewed regarding known somatic mutations or SNPs with the open source online tool VarSome (Kopanov et al., 2018).

2.6.7 Single Amplicon Validation

Detected mutation frequencies below 3% were validated with single amplicons covering the gene locus of interest using the Amplicon Library Preparation (Fusion Method) technology by Thermo Fisher Scientific. Hereby, oligonucleotide primers were individually designed with Primer3 software producing amplicons of about 150 – 200 bp in size (Untergasser et al., 2012). An Ion Xpress™ barcoding adapter and a tag sequence of additional 67 bp were attached to the 5' ends of the designed oligonucleotide primers. Amplification and sequencing were done in accordance with the manufacturer.

2.7 Blood Count

Information on haemoglobin (Hb) concentrations and the count of platelets were collected from patient files in close collaboration with Dr. med. Dominik Nann. Blood counts were obtained from the first day of hospitalisation, in which the bone marrow was extracted during the stay. Thresholds for anaemia and thrombocytopenia are in accordance with WHO guidelines (Organization, 2011). According to the classification, anaemic Hb levels are graded into mild (♂ 11.0 – 12.9 g/dL, ♀ 11.0 – 11.9 g/dL), moderate (♂/♀ 8.0 – 10.9 g/dL) and severe (♂/♀ <8.0 g/dL). Furthermore, thrombocytopenia was considered on platelet counts below $150 \times 10^3/\mu\text{L}$, while counts of $450 \times 10^3/\mu\text{L}$ or above were considered as thrombocytosis.

2.8 Statistical Analysis

Different groups of cases with and without mutations within *IDH2*, *RHOA*, *TET2* and *DNMT3A* were compared with each other using the Fisher's exact test. All statistical tests were two-sided and p-values < 0.05 were considered as significant. Statistical analysis on clinical parameters, including haemoglobin and platelet counts, were conducted with a two-sided t-test and considered as significant, if p-values < 0.05.

3 Results

3.1 Patient Characteristics

Thirty bone marrow biopsies of 22 different cases were initially included in this study for molecular analysis (**Table 4**). In 15/22 cases (68%), only one bone marrow sample and in 7/22 cases (32%), two or even three samples were available. The analysed cases corresponded to 12 female and 10 male patients (F:M 1.2:1) with a median age of 68 years at onset of AITL (range of 47 – 83 years).

Table 4 Patient characteristics. All cases with diagnosed AITL including sex (M/F), age at onset in years and the number of bone marrow samples.

Case	Sex	Age years	Bone Marrow Samples
A	F	47	A
B	F	68	B.1, B.2
C	M	78	C
D	F	62	D
E	F	69	E.1, E.2, E.3
F	M	61	F.1, F.2
G	M	81	G.1, G.2
H	F	68	H
I	F	53	I
J	M	71	J
K	F	73	K
L	M	83	L
M	M	65	M
O	F	65	O
P	F	73	P.1, P.2
Q	M	72	Q.1, Q.2
R	M	64	R
S	F	73	S
T	M	60	T
U	F	72	U.1, U.2
V	M	62	V
W	F	50	W

3.2 Evaluation of Bone Marrow Quality

3.2.1 Microscopy

Every bone marrow biopsy in this study derives from routine diagnostics and was evaluated microscopically prior to sequencing experiments concerning tissue quality. In addition to that, the proportion of haematopoietic cells, as well as signs of lymphoma infiltration were assessed (**Figure 7, Table 5**).

All bone marrow biopsies showed good quality except Q.2, which revealed few tissue and was, therefore, excluded from further analysis. Concerning the cellularity, 4/29 (14%) samples showed a cellularity of less than 30%. Throughout all biopsies, the cellularity was ranging from 10 – 80% with a median value of 70%.

Overall, 5/29 (17%) samples showed lymphoma infiltration with demonstration of at least three different TFH markers. Additionally, 5/29 (17%) biopsies revealed at least suspicious lymphoma infiltration not fulfilling criteria of lymphoma diagnosis. Taken together, ten biopsies of nine different cases (9/22, 41%) revealed characteristics of lymphoma infiltration in this cohort.

As specimens were extracted at different time points during the disease, bone marrow sample differed strongly in this cohort compared with the dates of lymphoma diagnosis. The first biopsy of each case ranged from 4423 days before to 85 days after AITL diagnosis. The median age of the first sample was assessed with 3 days prior to lymph node biopsy. In 15/22 cases (68%) bone marrow biopsies were taken before the date of diagnosis due to other reasons.

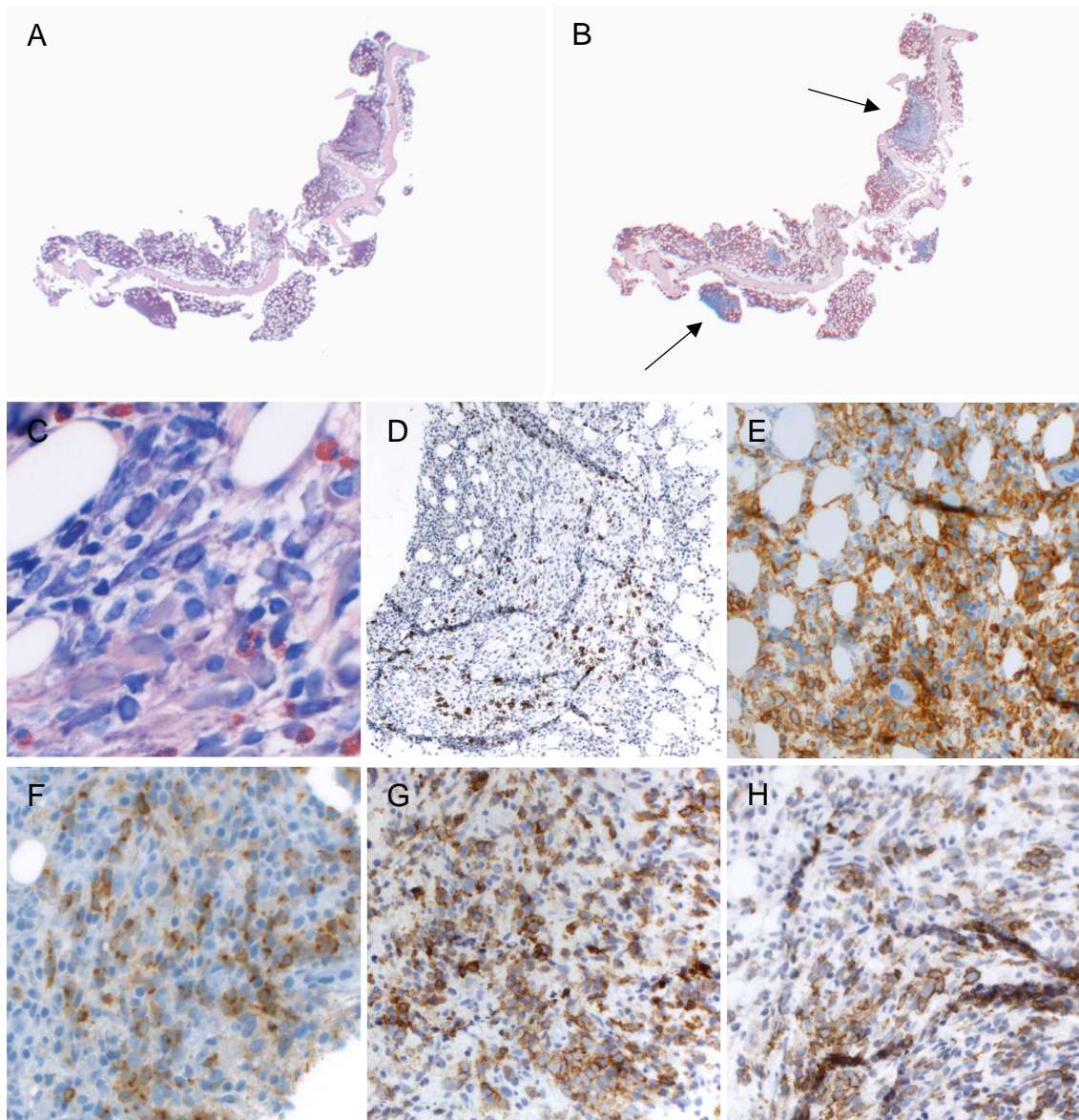


Figure 7 Representative AITL infiltration in bone marrow. For each case, cellularity, as well as signs of clear or suspicious/beginning lymphoma infiltration were assessed. The displayed specimen derives from case I, which was extracted one day prior to lymph node biopsy and AITL diagnosis. H&E stain shows a panoramic view of the bone marrow (**A**, 2,5X). The ASDC staining shows cellularity of 80%, whereas the paratrabeular lymphoma infiltration (blue clusters, arrows) is approximately 20% (**B**, 2,5X). The morphology of neoplastic cells is illustrated with Giemsa staining, neoplastic T-cells are small to medium size with clear to pale cytoplasm and irregular nuclei (**C**, 40X). The neoplastic cells were negative for B-cell markers such as CD20; however, a minor proportion of reactive B-cells shows positivity (**D**, 10X). Lymphoma cells were stained for T-cell markers such as CD4 (**E**, 20X). Moreover, neoplastic cells were stained positive for TFH immunophenotypic markers including CXCL13 (**F**, 20X), PD1 (**G**, 20X) and ICOS (**H**, 20X). The pictures were kindly provided by the Institute of Pathology and Neuropathology at the University Hospital of Tübingen, Germany.

3.2.2 DNA Integrity

Quantifiable concentrations of DNA could be extracted from all biopsies (29/29, 100%). Extracted DNA of bone marrow specimens were amplified by PCR and detected using gel electrophoresis to analyse integrity means of different amplifiable product sizes (**Figure 8**). Hereby, maximum amplicons ranged between 100 to 400 bp (**Table 5**). DNA of three bone marrow biopsies showed an integrity of 100 bp (3/29, 10%), another three of 200 bp (3/29, 10%), four of 300 bp (4/29, 14%) and 19 of 400 bp (19/29, 66%). DNA of 200 bp or less were treated with a kit to improve DNA integrity followed by generation of the NGS library.

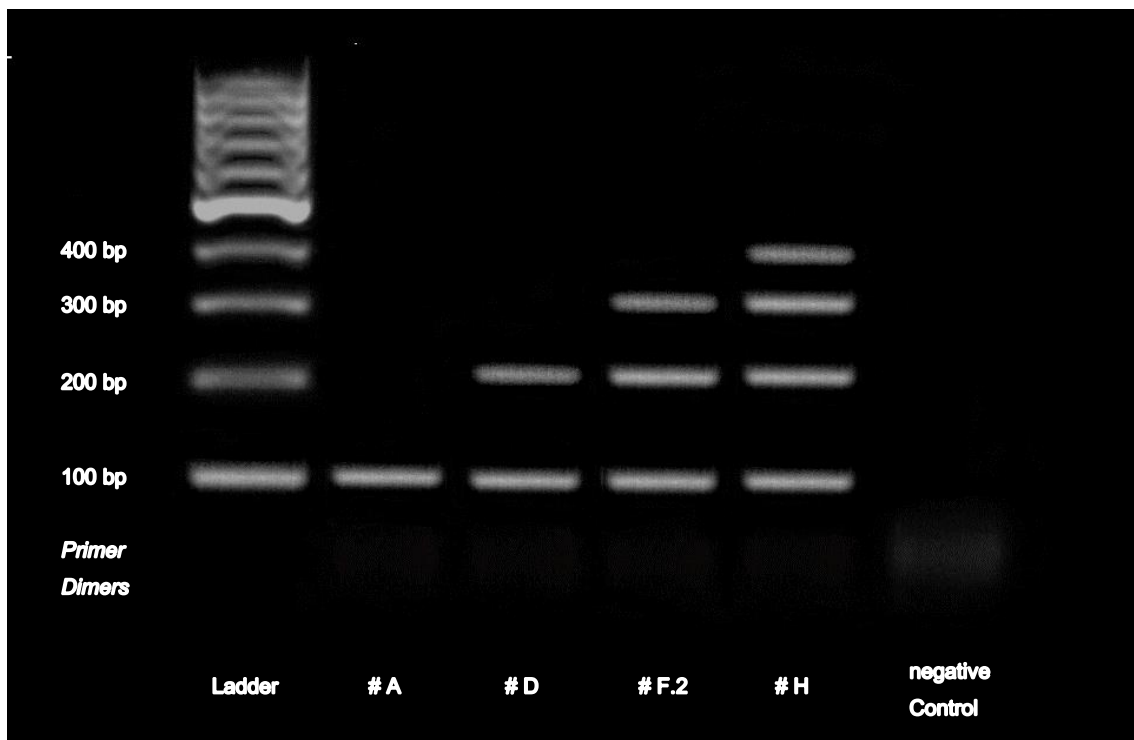


Figure 8 Representative picture of DNA integrity analysis. A polymerase-chain reaction (PCR) was conducted on all bone marrow biopsies to evaluate DNA quality prior to generation of libraries. After amplification, PCR products were transferred into a 2% agarose gel and ran at 180 V for about 20 min. Representative results of four different samples (A, D, F.2 and H) are shown above, including a 100-base pair (bp) DNA ladder and a negative control with water instead of DNA. Remaining oligonucleotide primers formed a slight band of primer dimers as seen with the negative control.

3.2.3 Final Sample Selection

The initial selection of 30 bone marrow biopsies was evaluated in terms of quality prior to further mutation analysis. Hereby, two aspects were considered, microscopical assessment and evaluation of DNA integrity. Only Q.2 was excluded from further analysis. This study includes a final selection of 29 bone marrow samples from 22 cases (**Figure 9**).

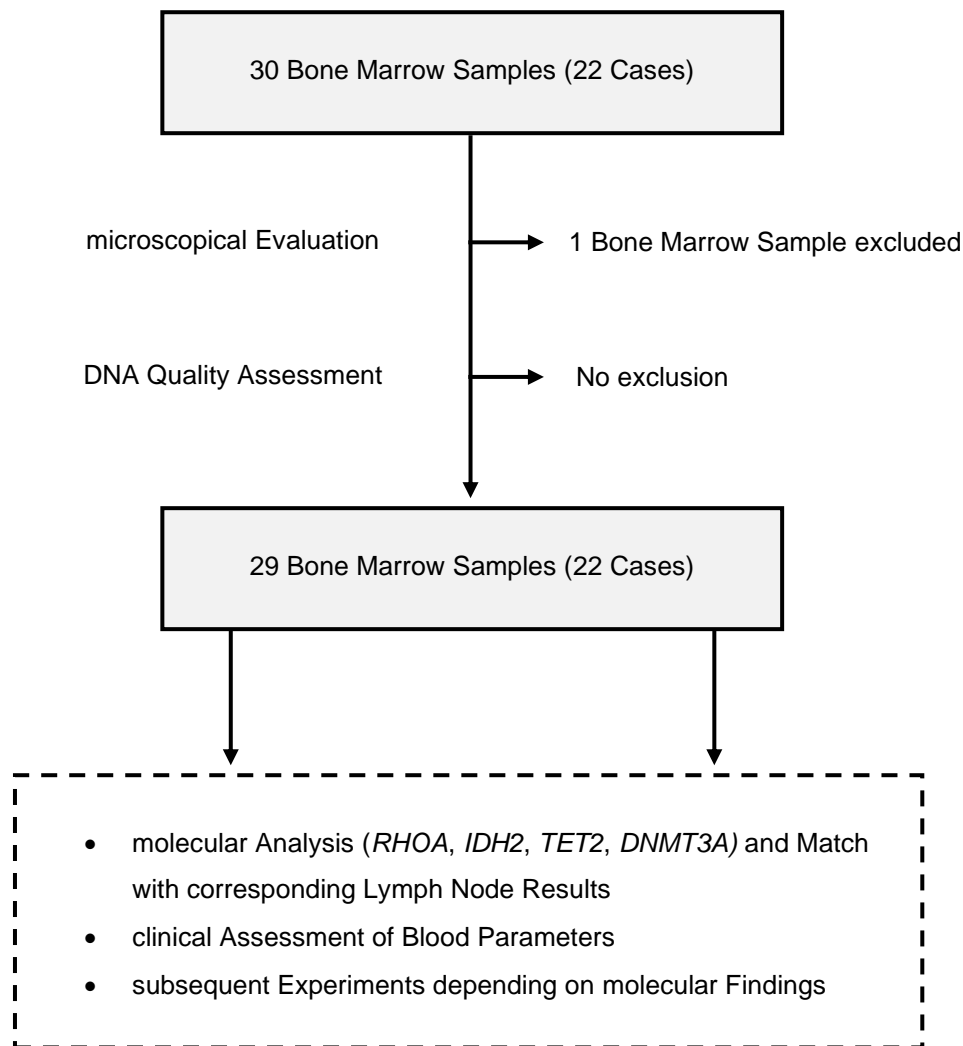


Figure 9 Selection process of bone marrow samples for further molecular analysis. 30 bone marrow biopsies of 22 patients were evaluated in terms of quality. Therefore, an initial assessment of the samples was conducted using microscopy, followed by a polymerase-chain reaction to proof DNA integrity. Finally, only one bone marrow specimen (Q.2) had to be excluded from further molecular analysis.

Table 5 Bone marrow quality characteristics. All cases with diagnosed AITL including sex, age at onset, the number of bone marrow biopsies, the sample age compared to the date of diagnosis, cellularity, microscopical lymphoma infiltration and the evaluated DNA integrity. Excluded samples are highlighted (shaded grey).

Case	Sex	Age years	Bone Marrow Sample	Sample Age days	Cellularity %	Lymphoma Infiltration	DNA Integrity bp
A	F	47	A	+4	40	-	100*
B	F	68	B.1	-7	80	-	300
			B.2	+241	70	-	100*
C	M	78	C	-329	10-20	+	400
D	F	62	D	+21	80	++	200*
			E.1	-1	70	++	400
E	F	69	E.2	+94	50	++	400
			E.3	+662	20-30	-	400
F	M	61	F.1	+27	80	-	400
			F.2	+184	20	-	300
G	M	81	G.1	-1270	60-70	-	400
			G.2	-7	80	+	400
H	F	68	H	-2	80	-	400
I	F	53	I	+1	80	++	400
J	M	71	J	-1	80	-	400
K	F	73	K	+12	60	-	400
L	M	83	L	-4	80	++	400
M	M	65	M	+15	30	+	300
O	F	65	O	-14	70	-	400
P	F	73	P.1	-4423	30-40	-	200*
			P.2	-12	50	-	400
Q	M	72	Q.1	-30	70	-	300
			Q.2		n.d.		100
R	M	64	R	+85	80	-	200*
S	F	73	S	-5	50	-	400
T	M	60	T	-23	20	+	400
U	F	72	U.1	-395	70	-	400
			U.2	-149	60-70	-	400
V	M	62	V	-316	70	-	400
W	F	50	W	-1	60-70	+	400

male (M) / female (F)

* pretreated with DNA Repair Kit before NGS library generation

no evidence (-), suspicious/beginning (+) and clear (++) bone marrow infiltration

not detectable (n.d.)

base pairs (bp)

3.3 Molecular Analysis

3.3.1 Quality of Next-Generation Sequencing

Prior to evaluation of mutations of each individual case, sequencing was evaluated concerning the amplicon and readout quality; however, NGS of DNA from the whole patient collective was accomplished successfully in terms of evaluability (**Table 6**). The first aspect, hereby, represents the uniformity of amplicon coverage, which was ranging from 86.44% (sample M) to a maximum of 98.92% (sample B.2). The median coverage throughout the project was determined with 98.31%. Another NGS characteristic, the average amplicon reading end-to-end, was accomplished with 98.13%, while the lowest value was 96.61% (sample B.1) and two samples even showed complete full-length amplicon reading (samples E.1, E.3). Finally, the average reads per amplicon were ranging from 849 (sample Q.1) to 28580 (sample K). Herein, the median value was assessed with 4134 average reads per amplicon. Throughout all experiments, two out of 118 amplicons were remarked with less than 100 reads.

Overall, five biopsies showed DNA integrity of 200 bp or less and were, therefore, treated with a DNA repair kit prior to library generation. Quality characteristics of amplicon libraries deriving from these samples did not show any differences compared to biopsies with higher DNA integrity (**Figure 10**). Uniformity of amplicon coverage and amplicon reading end-to-end was without any differences between both groups concerning mean values. Regarding average reads per amplicon, libraries from DNA of 200 bp or less were ranging from 3033 (sample B.2) to 6715 (sample D), while average reads per amplicons of untreated DNA ranged from 849 (sample Q.1) to 28580 (sample K).

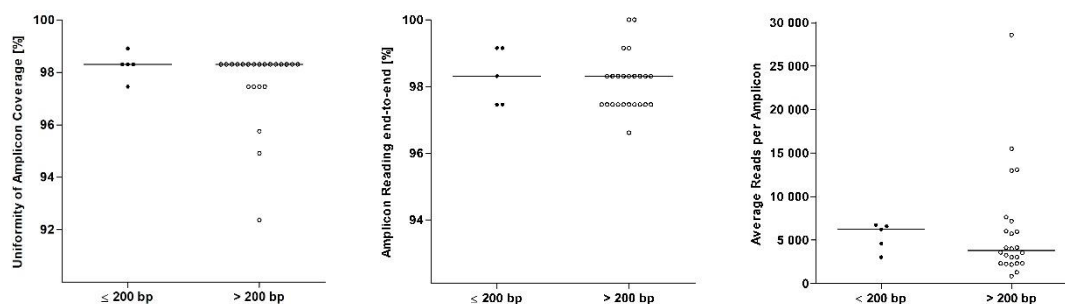


Figure 10 NGS quality characteristics. Amplicon libraries were successfully generated with DNA of all bone marrow biopsies (n=29). Libraries were evaluated prior to NGS analysis concerning uniformity of amplicon coverage (A), amplicon reading end-to-end (B) and the average reads per amplicon (C). DNA samples showing an integrity of 200 bp or less (n=5) were treated with a repair kit in advance to library generation. The horizontal line marks the median value for each graph not showing any difference compared to DNA of more than 200 bp DNA integrity (n=24).

Table 6 NGS quality characteristics. Quality characteristics in NGS analysis featuring the uniformity of amplicon coverage, amplicon reading end-to-end and the average reads per amplicon.

Case	Bone Marrow Sample	DNA Integrity <i>bp</i>	Uniformity of Amplicon Coverage %	Amplicon Reading end-to-end %	Average Reads per Amplicon
A	A	100*	97.46	97.46	4609
B	B.1	300	98.31	96.61	2181
	B.2	100*	98.92	98.31	3033
C	C	400	98.31	98.31	5979
D	D	200*	98.31	97.46	6715
E	E.1	400	97.46	100	4122
	E.2	400	98.31	98.31	7636
	E.3	400	97.46	100	2328
F	F.1	400	92.37	98.31	4146
	F.2	300	98.31	97.46	7172
G	G.1	400	98.31	97.46	2314
	G.2	400	98.31	98.31	2251
H	H	400	98.31	97.46	6006
I	I	400	98.31	99.15	4006
J	J	400	98.31	98.31	5729
K	K	400	97.46	99.15	28580
L	L	400	98.31	97.46	12981
M	M	300	86.44	98.31	15488
O	O	400	98.31	99.15	3585
P	P.1	200*	98.31	99.15	6574
	P.2	400	98.31	97.46	3041
Q	Q.1	300	98.31	97.46	849
R	R	200*	98.31	98.31	6224
S	S	400	98.31	97.46	2328
T	T	400	98.31	97.46	3052
U	U.1	400	95.76	98.31	1286
	U.2	400	94.92	97.46	13082
V	V	400	97.46	97.46	3274
W	W	400	98.31	98.31	3527

male (M) / female (F)

* pretreated with DNA Repair Kit before NGS library generation

base pairs (bp)

3.3.2 Genetic Findings

NGS was conducted on all samples concerning *IDH2*^{R172}, *RHOA*^{G17V}, *TET2* and *DNMT3A* mutation status. Hereby, amplicon libraries of each case were analysed with the Integrative Variant Caller software (**Figure 11**). All cases were assorted to subgroups concerning findings of *RHOA*^{G17V} and *IDH2*^{R172} within DNA of AITL lymph node biopsies. Group 1 encompasses a total of six cases, which all carried *IDH2*^{R172} and *RHOA*^{G17V}. Group 2 includes eight cases only revealing *RHOA*^{G17V}. Finally, group 3 represents eight cases with wildtype configuration concerning both genes (**Table 7**). A detailed table including precise genetic findings in lymph nodes and corresponding bone marrow specimens is shown in **Table 8**.

In group 1, six cases revealed *IDH2*^{R172} in neoplastic cells from lymph node biopsies. As opposed to this, the mutation was present in corresponding bone marrow of 1/6 (17%) cases. Only sample E.1 showed *IDH2*^{R172} in bone marrow with a VAF of 7%, but also reflected clear lymphoma infiltration microscopically.

Furthermore, group 1 and 2 together include 14 cases with confirmed *RHOA*^{G17V} in lymph node biopsies. Mutations were present within bone marrow in only 2/14 (14%) cases of these subgroups, samples E.1 (VAF 0.9%) and I (VAF 2%). Sample I; however, showed similar features of lymphoma infiltration microscopically as seen in E.1.

Overall, mutations within *TET2* existed in lymph node specimen of 19/22 (86%) cases throughout all three groups. In bone marrow, 17/22 (77%) cases carried mutations within *TET2*. Only 2/19 (11%) cases with *TET2* mutations in lymph nodes were not present in bone marrow. Most interestingly, each mutation within bone marrow also existed in corresponding lymph node specimens, regardless whether lymphoma infiltration could be detected or not. Focussing on the *RHOA*^{G17V} subgroups 1 and 2, 13/14 (93%) cases displayed mutated *TET2*, whereas only 4/8 (50%) cases in group 3 showed a mutation. There is no significant difference between group 1 and 2 concerning *TET2* mutations; however, the difference of *TET2* mutations in all *RHOA*^{G17V} cases (groups 1 and 2) compared with *RHOA* wildtype cases (group 3) is statistically significant ($p=0.03$) using the Fisher's exact test.

Mutated *DNMT3A* was present in 10/22 (45%) AITL affected lymph nodes. In bone marrow, 11/22 (50%) cases revealed mutations; however, only 9/22 (41%) cases carried the same mutation in bone marrow and lymph node specimens. Statistically significant differences between the occurrence of *DNMT3A* mutations within any of the three subgroups did not exist using the Fisher's exact test.

Focussing on groups 1 and 2, 14/14 (100%) cases revealed mutations in *DNMT3A* and/or *TET2* in bone marrow, as well as in the corresponding lymph node specimen. In contrast to that, group 3 only showed a matching mutation profile concerning either of these two genes in 4/8 (50%) cases. Furthermore, 8/22 (36%) cases carried coexisting *DNMT3A* and *TET2* mutations.

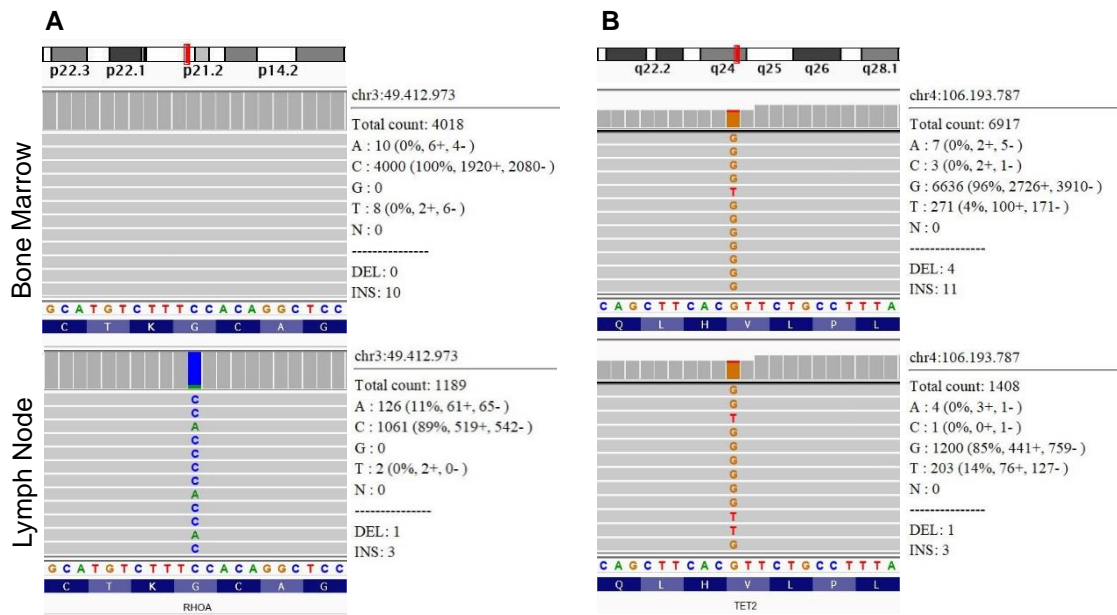


Figure 11 Representative mutational findings analysed with the Integrative Variant Caller. Each horizontal, bar (grey) represents one sequence read, which was aligned to the hg19 reference genome. A brief extract from the chromosomal map is shown above as well to indicate the chromosomal locus. The precise genetic location, the total count of amplicon reads, as well as the individual calls for each base are shown next to the graphs, including information on distribution into sense (+) and antisense (-) strands. Genetic variants, which appeared more often than 1% of the total count were automatically called and highlighted. For instance, case H showed the variant c.50C>A in 126 out of 1189 reads (11%) from lymph node DNA, which leads to the mutation *RHOA*^{G17V}. In DNA from bone marrow; however, 100% showed wildtype configuration (A). Concerning *TET2*, both specimens revealed the variant c.4249G>T, which results in *TET2*^{V1417F} (B).

Table 7 Genetic profiles of subgroups. Mutations of bone marrow samples and corresponding lymph nodes (LN) are shown concerning *IDH2^{R172}*, *RHOA^{G17V}*, *TET2* and *DNMT3A*. The age of bone marrow extractions is included as well as the microscopical lymphoma infiltration.

	Case	Sample	Age of Sample days*	Infiltration	<i>IDH2^{R172}</i>	<i>RHOA^{G17V}</i>	<i>TET2</i>	<i>DNMT3A</i>
Group 1: <i>RHOA</i> and <i>IDH2</i> mutated	A	LN						
		A	+4					
	B	B.1	-7					
		LN						
	C	B.2	+241					
		C	-329	+				
	D	LN						
		D	+21	++				
	E	E.1	-1	++				
		LN						
		E.2	+94					
	F	E.3	+662					
		LN						
		F.1	+27					
	F.2	+184						

Group 2: <i>RHOA</i> mutated, <i>IDH2</i> wildtype	G	G.1	-1260					
		G.2	-7	+				
		LN						
	H	H	-2					
		LN						
	I	I	+1	++				
		LN						
	J	J	-1					
		LN						
	K	K	+12					
		LN						
	L	L	-4	++				
		LN						
	M	M	+15	+				
LN								
O	O	-14						
	LN							

Group 3: <i>RHOA</i> and <i>IDH2</i> wildtype	P	P.1	-4423					
		P.2	-12					
		LN						
	Q	Q	-30					
		LN						
	R	R	+85					
		LN						
	S	S	-5					
		LN						
	T	T	-23	+				
		LN						
	U	U.1	-395					
		U.2	-149					
		LN						
	V	V	-316					
		LN						
W	W	-1	+					
	LN							







	<i>IDH2^{R172}</i>		<i>TET2</i> mutated	+	suspicious/beginning Infiltration
	<i>RHOA^{G17V}</i>		<i>DNMT3A</i> mutated	++	clear Infiltration
	Wildtype		Lymph Node (LN)	*	compared to lymph node (diagnosis)

Table 8 Genetic variants. Genetic variants in DNA of bone marrow samples (dark blue) and corresponding lymph nodes (LN, bright blue) regarding *IDH2*^{R172}, *RHOA*^{G17V}, *TET2* and *DNMT3A*. Mutations are shown including the variant allelic frequency (VAF) and the VarSome (VS) prediction. Genetic findings of low frequency were verified by single amplicon validation (bold).

Case	Sample	<i>IDH2</i> ^{R172}		<i>RHOA</i> ^{G17V}		<i>TET2</i>			<i>DNMT3A</i>		
		Mutation	VAF	Mutation	VAF	Mutation	VAF	VS	Mutation	VAF	VS
A	LN	c.514A>G, p.R172G	8%	c.50G>T, p.G17V	7%	c.2332C>T, p.Q778* c.4501C>T, p.Q1501*	44% 10%	P P	-	-	-
	A	-	-	-	-	c.2332C>T, p.Q778*	44%	P	-	-	-
B	LN	c.516G>T, p.R172S	5%	c.50G>T, p.G17V	4%	c.3224A>G, p.D1075G c.4038delT, p.N1346fs	49% 12%	US LP	c.2645G>A, p.R882H	10%	P
	B.1	-	-	-	-	c.3224A>G, p.D1075G c.4038delT, p.N1346fs	50% 1%	US LP	c.2645G>A, p.R882H	0.8%	P
	B.2	-	-	-	-	c.3224A>G, p.D1075G	44%	US	c.2645G>A, p.R882H	0.4%	P
C	LN	c.515G>A, p.R172K	17%	c.50G>T, p.G17V	19%	c.3088C>T, p.Q1030*	39%	P	-	-	-
	C	-	-	-	-	c.3088C>T, p.Q1030*	46%	P	-	-	-
D	LN	c.515G>C, p.R172T	3%	c.50G>T, p.G17V	4%	c.2754_2761del, p.R918fs c.4210C>T, p.R1404*	6% 6%	P P	c.2469_2470insG, p.I824fs	6%	P
	D	-	-	-	-	c.2754_2761del, p.R918fs	1%	P	-	-	-
E	LN	c.516G>T, p.R172S	7%	c.50G>T, p.G17V	9%	c.5399_5400insT, p.M1800fs c.4503_4504del, p.Q1501fs	19% 11%	P LP	-	-	-
	E.1	c.516G>T, p.R172S	1%	c.50G>T, p.G17V	0.9%	c.5399_5400insT, p.M1800fs c.4503_4504del, p.Q1501fs	5% 2%	P LP	-	-	-
	E.2	-	-	-	-	c.5399_5400insT, p.M1800fs c.4503_4504del, p.Q1501fs	4% 1.6%	P LP	c.1925G>T, p.G642V	1%	LP
	E.3	-	-	-	-	c.5399_5400insT, p.M1800fs c.4503_4504del, p.Q1501fs	10% 8%	P LP	c.1925G>T, p.G642V	2.7%	LP
F	LN	c.516G>T, p.R172S	3%	c.50G>T, p.G17V	5%	c.3810_3817del, p.C1271fs c.3867T>G, p.C1289W	19% 8%	P LP	c.1755_1756insG, p.C586fs c.2206C>T, p.R736C	20% 0.9%	P LP
	F.1	-	-	-	-	c.3810_3817del, p.C1271fs c.3867T>G, p.C1289W	18% 0.3%	P LP	c.1755_1756insG, p.C586fs c.2206C>T, p.R736C	10% 3.3%	P LP
	F.2	-	-	-	-	c.3810_3817del, p.C1271fs c.3867T>G, p.C1289W	12% 0.2%	P LP	c.1755_1756insG, p.C586fs c.2206C>T, p.R736C	12% 3.4%	P LP
G	LN	-	-	c.50G>T, p.G17V	11%	c.3782G>C, p.R1261P c.3893delG, p.C1298fs	31% 12%	LP P	c.1304_1305insT, p.Y436fs	29%	P
	G.1	-	-	-	-	c.3782G>C, p.R1261P	45%	LP	c.1304_1305insT, p.Y436fs	43%	P
	G.2	-	-	-	-	c.3782G>C, p.R1261P c.3893delG, p.C1298fs	46% 0.4%	LP P	c.1304_1305insT, p.Y436fs	38%	P
H	LN	-	-	c.50G>T, p.G17V	10%	c.4249G>T, p.V1417F	15%	US	c.2645G>A, p.R882H	14%	P
	H	-	-	-	-	c.4249G>T, p.V1417F	3.9%	US	c.2645G>A, p.R882H	3%	P
I	LN	-	-	c.50G>T, p.G17V	18%	c.3812G>A, p.C1271Y	48%	LP	c.976C>T, p.R326C	24%	US
	I	-	-	c.50G>T, p.G17V	2%	c.3812G>A, p.C1271Y	7%	LP	c.976C>T, p.R326C	3%	US
J	LN	-	-	c.50G>T, p.G17V	2%	c.786T>A, p.C262*	2%	P	c.976C>T, p.R326C c.2711C>T, p.P904L	4% 0.5%	US P
	J	-	-	-	-	-	-	-	c.976C>T, p.R326C c.2711C>T, p.P904L	18% 1.4%	US P
K	LN	-	-	c.50G>T, p.G17V	15%	c.3658_3677del, p.T1220fs c.3824G>T, p.G1275V	21% 18%	P US	-	-	-
	K	-	-	-	-	c.3658_3677del, p.T1220fs	0.3%	P	-	-	-
L	LN	-	-	c.50G>T, p.G17V	3%	c.840_841insT, p.N281* c.4854C>G, p.Y1618*	37% 37%	P P	c.1296delC, p.Y432*	38%	P
	L	-	-	-	-	c.840_841insT, p.N281* c.4854C>G, p.Y1618*	44% 44%	P P	c.1296delC, p.Y432*	43%	P
M	LN	-	-	c.50G>T, p.G17V	4%	c.1720C>T, p.Q574* c.5582G>A, p.G1861E	9% 8%	P US	-	-	-
	M	-	-	-	-	c.1720C>T, p.Q574* c.5582G>A, p.G1861E	0.9% 0.3%	P US	-	-	-

O	LN	-	-	c.50_51delGA insTT, p.G17V	4%	c.3796A>T, p.N1266Y c.5650A>G, p.T1884A	37% 33%	US P	-	-	-
	O	-	-	-	-	c.3796A>T, p.N1266Y c.5650A>G, p.T1884A	48% 44%	US P	c.1603_1604ins#, p.Y528_Q534dup	37%	LP
P	LN	-	-	-	-	c.3788G>A, p.C1263Y	20%	US	c.2645G>A, p.R882H	21%	P
	P.1	-	-	-	-	c.3788G>A, p.C1263Y	3%	US	c.2645G>A, p.R882H	1.9%	P
	P.2	-	-	-	-	c.3788G>A, p.C1263Y	4%	US	c.2645G>A, p.R882H	4%	P
Q	LN	-	-	-	-	-	-	-	-	-	-
	Q.1	-	-	-	-	-	-	-	-	-	-
R	LN	-	-	-	-	c.2924G>C, p.S975T	26%	US	-	-	-
	R	-	-	-	-	-	-	-	-	-	-
S	LN	-	-	-	-	c.2759delT, p.L920* c.5527_5530dup, p.D1844fs	36% 34%	LP P	-	-	-
	S	-	-	-	-	c.2759delT, p.L920* c.5527_5530dup, p.D1844fs	41% 44%	LP P	-	-	-
T	LN	-	-	-	-	-	-	-	-	-	-
	T	-	-	-	-	-	-	-	-	-	-
U	LN	-	-	-	-	c.2599T>C, p.Y867H c.5680C>A, p.P1894T c.2919C>A, p.C973*	51% 40% 39%	LB US LP	c.912del, p.W305fs c.1443C>A, p.Y481* c.1031T>C, p.L344P	40% 0.5% 0.2%	P P LP
	U.1	-	-	-	-	c.2599T>C, p.Y867H c.5680C>A, p.P1894T c.2919C>A, p.C973*	46% 16% 5%	LB US LP	c.912del, p.W305fs c.1443C>A, p.Y481* c.1031T>C, p.L344P	14% 8% 3%	P P LP
	U.2	-	-	-	-	c.2599T>C, p.Y867H c.5680C>A, p.P1894T c.2919C>A, p.C973*	50% 18% 10%	LB US LP	c.912del, p.W305fs c.1443C>A, p.Y481* c.1031T>C, p.L344P	19% 5% 1.6%	P P LP
	U.3	-	-	-	-	c.2599T>C, p.Y867H c.5680C>A, p.P1894T c.2919C>A, p.C973*	50% 18% 10%	LB US LP	c.912del, p.W305fs c.1443C>A, p.Y481* c.1031T>C, p.L344P	19% 5% 1.6%	P P LP
V	LN	-	-	-	-	c.2862G>A, p.W954*	54%	P	-	-	-
	V	-	-	-	-	c.2862G>A, p.W954*	14%	P	-	-	-
W	LN	-	-	-	-	-	-	-	-	-	-
	W	-	-	-	-	-	-	-	-	-	-

#ACGACGACGACGGCTACCACT (case O, DNMT3A)

VarSome (VS) prediction: pathogenic (P)
likely pathogenic (LP)
uncertain significance (US)
likely benign (LB)

3.3.3 *TET2* Mutations

As mentioned previously, 17/22 (77%) cases carried at least one *TET2* mutation within bone marrow, which was also detected in the lymph node. Only cases J and R revealed a mutation, which existed in the lymphoma DNA, that was not present in the bone marrow. Overall, 8/17 (47%) cases carried one, 8/17 (47%) carried two and 1/17 (6%) case carried even three different *TET2* mutations. Apart from the matching mutations, four additional mutations existed within lymphoma DNA, which did not exist in bone marrow specimen.

Interestingly, 27 different *TET2* mutations existed in this study cohort; however, no single mutation appeared more than once. Ten of 27 (37%) mutations were located upstream of functional domains and predominantly nonsense mutations. In contrast to that, 8/27 (30%) mutations were located inside the cysteine-rich domain and 9/27 (33%) inside the double-stranded β helix domain and mainly missense and frameshift mutations (**Figure 12**). All mutations are predicted to be loss-of-function mutations.

Variant allelic frequencies were evaluated for each mutation ranging from 0.2 – 50% in bone marrow and 2 – 54% in lymph nodes (**Figure 13**). A subgroup of cases, including A, B, C, G, L, O, S and U showed mutation frequencies of even 44 – 50%. Interestingly, VAF of *TET2* mutations were higher in bone marrow than any other coexisting mutation within *IDH2*, *RHOA* or *DNMT3A*. Case J was the only exception, which showed wildtype configuration of *TET2*.

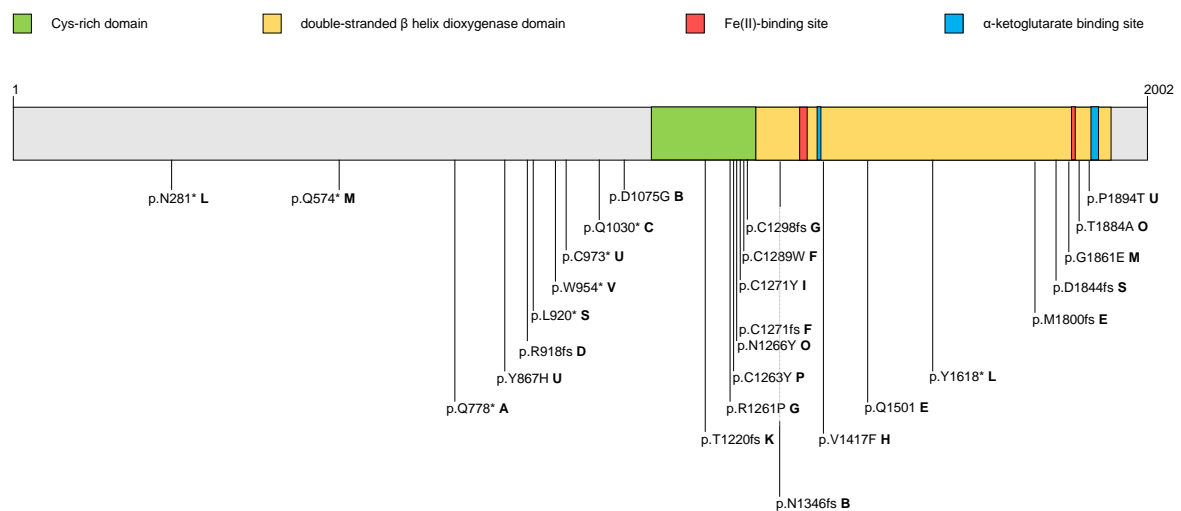


Figure 12 Schematic protein structure of *TET2* including the mutation site of patients with AITL.

Each identified mutation, which was present in bone marrow and neoplastic tissue, is marked on the map above including the mutation as well as the case (bold letter). Interestingly, no single mutation existed in more than one case. Overall, 27 different mutations existed, most commonly missense mutations, but also nonsense (*) and frameshift (fs) mutations.

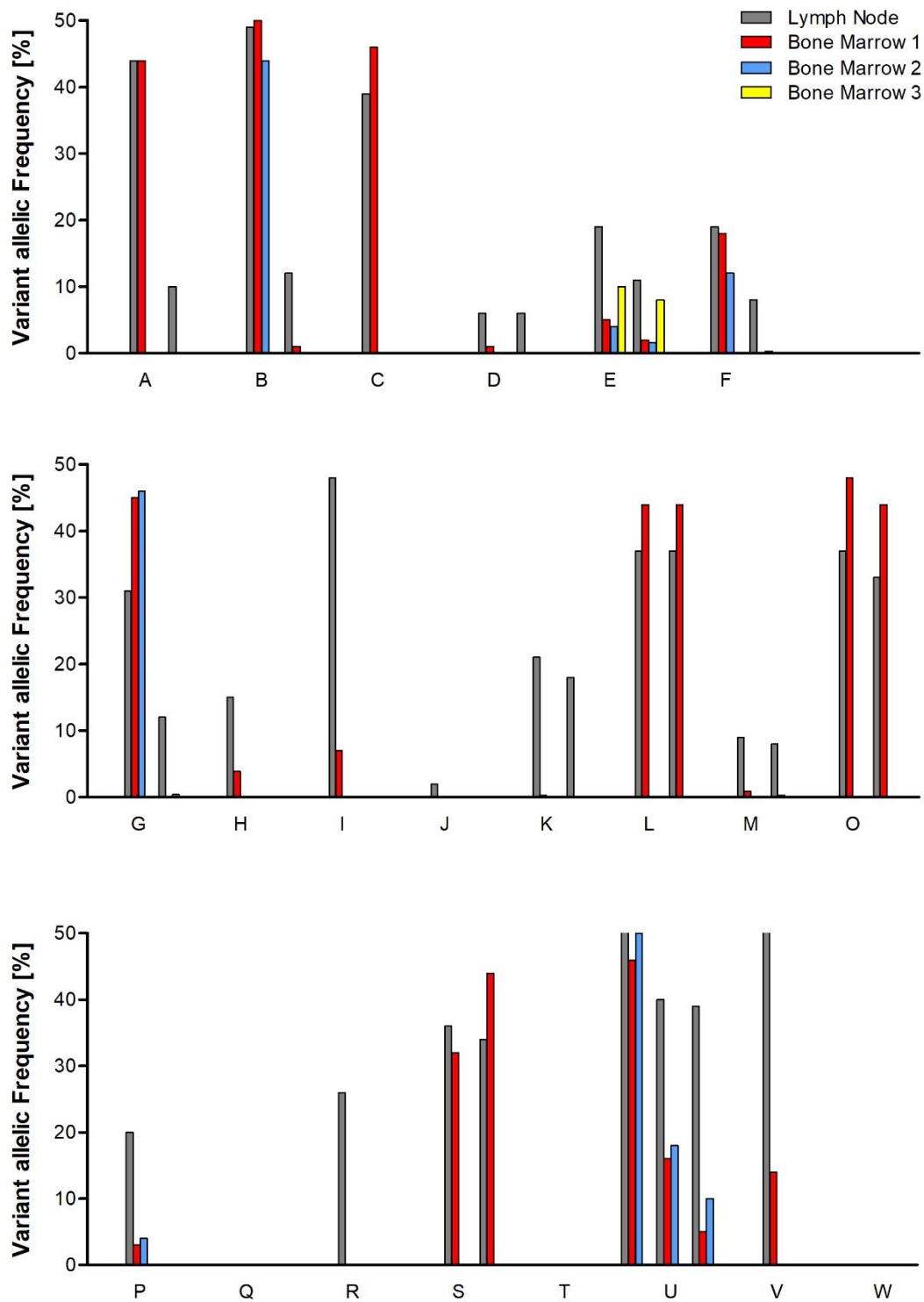


Figure 13 Variant allelic frequencies in *TET2*. Variant allelic frequencies of *TET2* are demonstrated for each biopsy. Samples are grouped according to the mutation profile of the lymph node biopsies concerning *IDH2^{R172}* and *RHOA^{G17}* (**A** *IDH2^{R172}/RHOA^{G17TV}*, **B** *IDH2^{wt}/RHOA^{G17TV}*, **C** *IDH2^{wt}/RHOA^{wt}*). The number of bar groups indicate the number of different *TET2* mutations. Overall, 17 bone marrow specimens showed at least one *TET2* mutation, which all could be identified in corresponding lymph nodes.

3.3.4 DNMT3A Mutations

Although 11/22 (50%) cases revealed genetically altered *DNMT3A* within bone marrow, only nine cases carried the same mutation as in the lymph node. Six of nine (67%) cases carried only one, 2/9 (22%) carried two and 1/9 (11%) case carried three different genetic alterations. While most variants were unique for each case, *DNMT3A*^{R882H} (3/9, 33%) and *DNMT3A*^{R326C} (2/9, 22%) existed in multiple cases.

Overall, ten different mutations existed in this study cohort (**Figure 14**). Three of ten (30%) mutations were located inside the PWWP-, 3/10 (30%) within the catalytic and 1/10 (10%) within the ADD-domain. All these mutations were either frameshift or missense mutations. In contrast to that, 3/10 (30%) mutations were not directly located within a functional domain and exclusively nonsense mutations. All mutations were predicted to be pathogenic and loss-of-function mutations. Variant allelic frequencies were evaluated for each mutation ranging from 0.4 – 43% in bone marrow and 0.2 – 40% in lymph nodes (**Figure 15**).

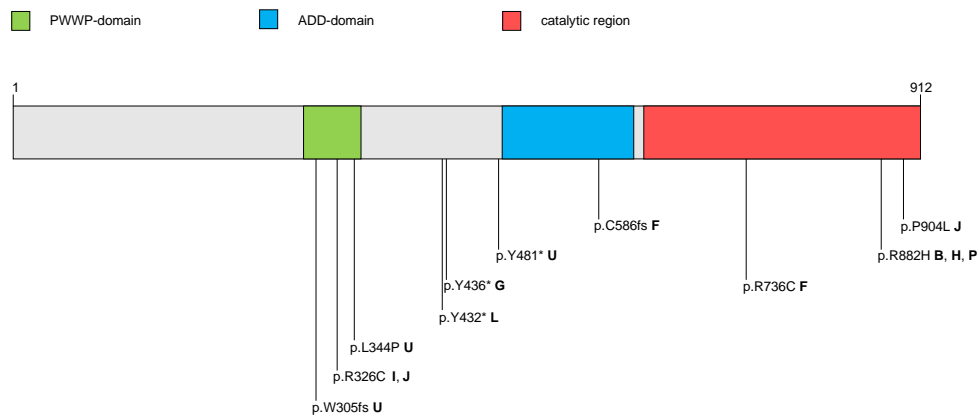


Figure 14 Schematic protein structure of *DNMT3A* including the mutation site of patients with AITL. Each identified mutation, which was present in bone marrow and neoplastic tissue, is marked on the map above including the precise mutation as well as the case (bold letter). Overall, ten different mutations existed, most commonly missense mutations, but also nonsense (*) and frameshift (fs) mutations. *DNMT3A*^{R882H} existed in three different cases and represented the most common mutation within the study cohort.

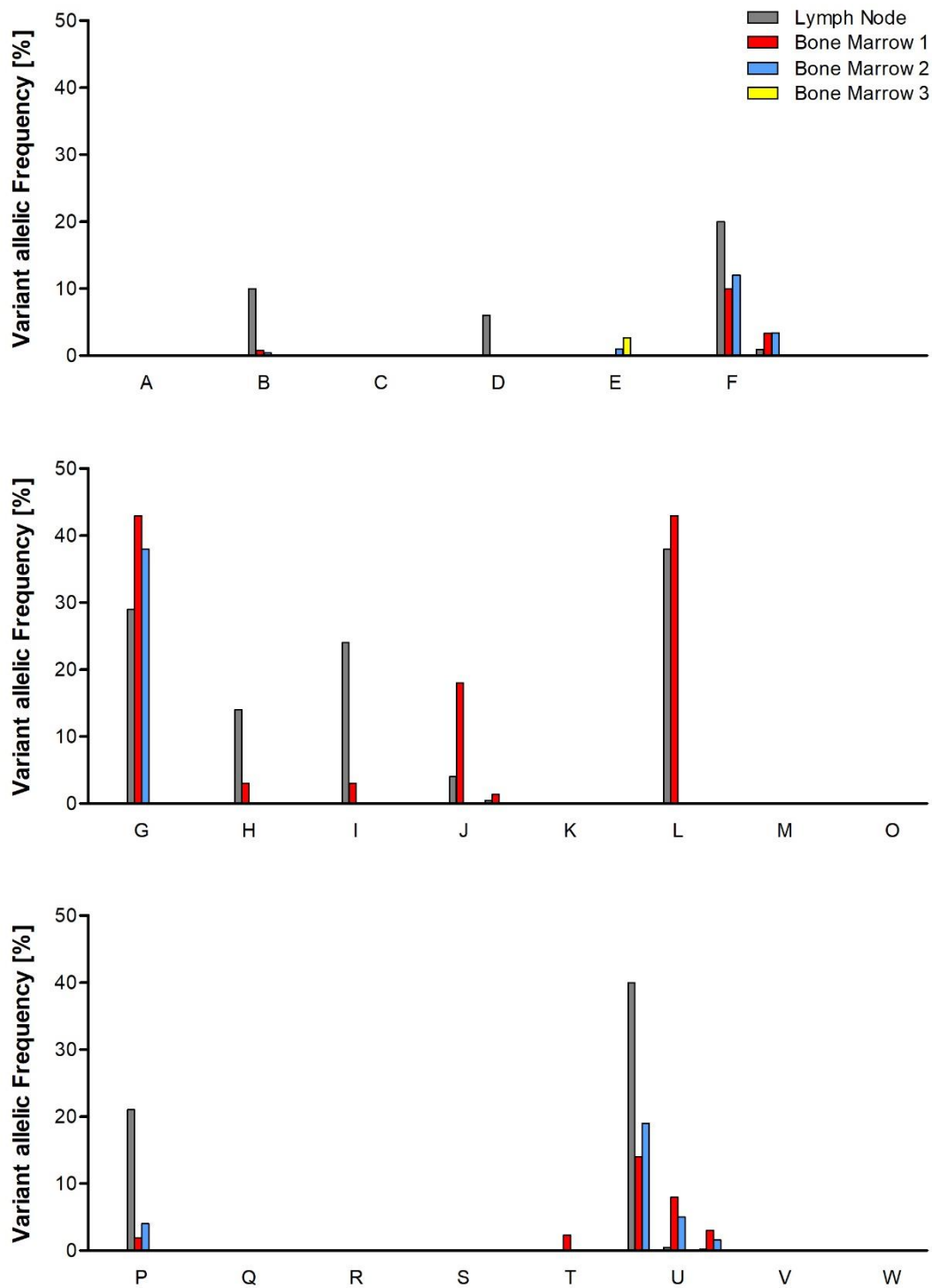


Figure 15 Variant allelic frequencies in DNMT3A. Variant allelic frequencies of DNMT3A are demonstrated for each biopsy. Samples are grouped according to the mutation profile of the lymph node biopsies concerning *RHOA*^{G17V} and *IDH2*^{R172} (**A** *RHOA*⁺/*IDH2*⁺, **B** *RHOA*⁺/*IDH2*^{wt}, **C** *RHOA*^{wt}/*IDH2*^{wt}). The number of bar groups indicate the number of different DNMT3A mutations. Overall, eight bone marrow specimens showed at least one DNMT3A mutation, which all could be identified in corresponding lymph nodes.

3.4 Examination of Germline Variants

Some cases showed high VAF of *TET2* and *DNMT3A* mutations in bone marrow, which were suspicious for germline variants. In order to investigate possible germline mutations, DNA from FFPE non-haematopoietic tissue was extracted from three representative AITL patients and analysed using NGS (**Table 9**). Case A revealed one *TET2* mutation in DNA from bone marrow with a VAF of 44%, which also existed in 8% of DNA deriving from an ileum biopsy. Case L possessed two *TET2* mutations of 44% each and one mutation in *DNMT3A* with 43% in DNA of the bone marrow. All three mutations existed in the duodenal biopsy, but VAF was less with only 4 – 7%. Finally, case S showed one suspicious mutation in *TET2* with VAF of 44%; however, this mutation was present in DNA from a stomach specimen with only 0.8%.

Table 9 Evaluation of germline variants. DNA of three representative patients was extracted from non-haematopoietic FFPE tissue (green) and sequenced using the AITL panel. Biopsies of normal tissue derive from ileum (A), duodenum (L) and stomach (S). Genetic profile considering *RHOA*^{G17V}, *IDH2*^{R172}, *TET2* and *DNMT3A* are demonstrated including the variant allelic frequency (VAF), as well as mutational findings in corresponding bone marrow samples (blue).

Case	Sample	<i>IDH2</i> ^{R172}		<i>RHOA</i> ^{G17V}		<i>TET2</i>		<i>DNMT3A</i>	
		Mutation	VAF	Mutation	VAF	Mutation	VAF	Mutation	VAF
A	A	-	-	-	-	c.2332C>T, p.Q778*	44%	-	-
	ileum	-	-	-	-	c.2332C>T, p.Q778*	8%	-	-
L	L	-	-	-	-	c.840_841insT, p.N281* c.4854C>G, p.Y1618*	44% 44%	c.1296delC, p.Y432*	43%
	duodenum	-	-	-	-	c.840_841insT, p.N281* c.4854C>G, p.Y1618*	7% 6%	c.1296delC, p.Y432*	4%
S	S	-	-	-	-	c.2759delT, p.L920* c.5527_5530dup, p.D1844fs	32% 44%	-	-
	stomach	-	-	-	-	c.2759delT, p.L920* c.5527_5530dup, p.D1844fs	4% 0.8%	-	-

3.5 Examination of MDS Properties

3.5.1 Blood Count

After molecular analysis, all 22 cases were examined concerning clinical parameters, such as Hb and platelet levels (**Table 10**). Hereby, clinical parameters derived from initial blood counts of the hospitalisation, where bone marrow specimens were extracted during the in-patient stay. Only values of the first bone marrow sample of each case were considered. Overall, the mean Hb value was assessed with 11.2 g/dL. 9/22 (41%) cases showed mild, 6/22 (27%) moderate and 1/22 (5%) even severe anaemia. In contrast to that, 6/22 (27%) showed Hb levels within the physiological range. Considering platelet counts, the mean value was assessed with $236.8 \times 10^3/\mu\text{L}$. In this cohort, 2/22 (9%) cases showed thrombocytopenia and 2/22 (9%) thrombocytosis, while 18/22 (82%) revealed platelet counts within the reference range.

Higher VAF in *TET2* seems to correlate with lower Hb and platelet levels; however, neither correlation was significant (**Figure 16**). Although a trend could be seen, the goodness-of-fit R^2 was assessed with 0.164 for the correlation of VAF and Hb levels and even only 0.076 considering platelet counts. Interestingly, two subgroups in this cohort could be identified concerning VAF in *TET2*. While 14/22 (64%) cases revealed frequencies of 0 – 18%, 8/22 (36%) cases showed frequencies ranging from 44 – 50%. Both subgroups were compared with each other under clinical aspects, including Hb and platelet levels, as well as the age at blood extractions (**Figure 17**). The subgroup of low *TET2* VAF (<20%) was well balanced with seven female and seven male patients. The mean age was 63.8 years at the date of blood extraction. The mean Hb was 11.9 g/dL, while the mean platelet count was $258.1 \times 10^3/\mu\text{L}$. In contrast to that, the subgroup of high *TET2* VAF (>40%) comprised five female and three male patients with a mean age of 70.3 years at the date of blood extraction. The mean Hb value was determined with 10.1 g/dL, while the mean platelets were $199.4 \times 10^3/\mu\text{L}$. Although lower Hb and platelet counts, as well as a higher age during blood extraction, existed in the subgroup with higher *TET2* VAF, differences between both subgroups were not statistically significant.

Table 10 Blood counts. Initial blood counts of each case at clinical hospitalisation with subsequent bone marrow extraction. Values are listed below including the age at AITL onset, age at blood extraction (BE), haemoglobin (Hb) and platelet levels, as well as the variant allelic frequency (VAF) of the highest *TET2* mutation. According to the classification of the WHO, anaemic Hb levels are considered as mild (♂ 11.0 – 12.9 g/dL, ♀ 11.0 – 11.9 g/dL, +), moderate (♂/♀ 8.0 – 10.9 g/dL, ++) and severe (♂/♀ <8.0 g/dL, +++).

Case	Sex	Age at Onset years	Bone Marrow Sample	Sample Age Days	VAF <i>TET2</i> %	Age at BE years	Hb g/dL	Anaemia	Platelets 1000/ μ L
A	F	47	A	+4	44	47	12.3		344
B	F	68	B.1	-7	50	68	5.2	+++	170
C	M	78	C	-329	46	78	11.7	+	157
D	F	62	D	+21	1	62	12.8		356
E	F	69	E.1	-1	5	69	9.0	++	119
F	M	61	F.1	+27	18	61	12.0	+	243
G	M	81	G.1	-1270	45	77	7.8	+++	169
H	F	68	H	-2	3.9	68	11.8	+	156
I	F	53	I	+1	7	53	11.6	+	243
J	M	71	J	-1	0	71	13.7		198
K	F	73	K	+12	0.3	73	11.4	+	192
L	M	83	L	-4	44	83	12.3	+	47
M	M	65	M	+15	0.9	65	9.9	++	518
O	F	65	O	-14	48	65	12.2		167
P	F	73	P.1	-4423	3	62	14.4		215
Q	M	72	Q.1	-30	0	72	11.3	+	200
R	M	64	R	+85	0	65	14.8		240
S	F	73	S	-5	44	73	9.0	++	150
T	M	60	T	-23	0	60	11.6	+	456
U	F	72	U.1	-395	46	71	10.2	++	391
V	M	62	V	-316	14	62	12.9	+	264
W	F	50	W	-1	0	50	9.3	++	214

male (M) / female (F)

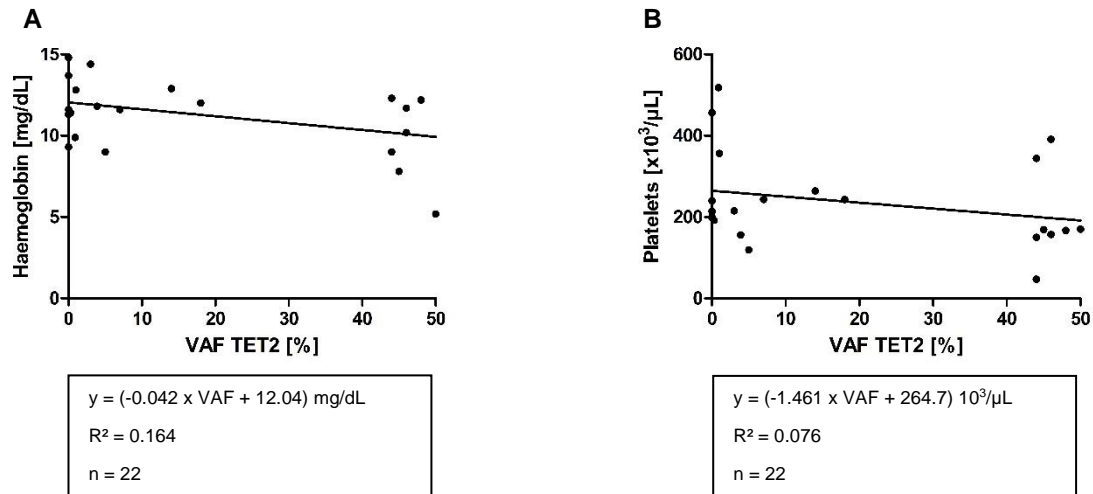


Figure 16 Correlation of blood parameters with *TET2* mutation frequencies. Haemoglobin (A) and platelet levels (B) were correlated with the variant allelic frequency (VAF) of *TET2* mutations. Clinical parameters derived from the initial blood counts of the hospitalisation, in which the first bone marrow was extracted during the in-patient stay. The equation of the regression line (y), as well the goodness-of-fit (R^2) and the number of values (n) are shown below both graphs.

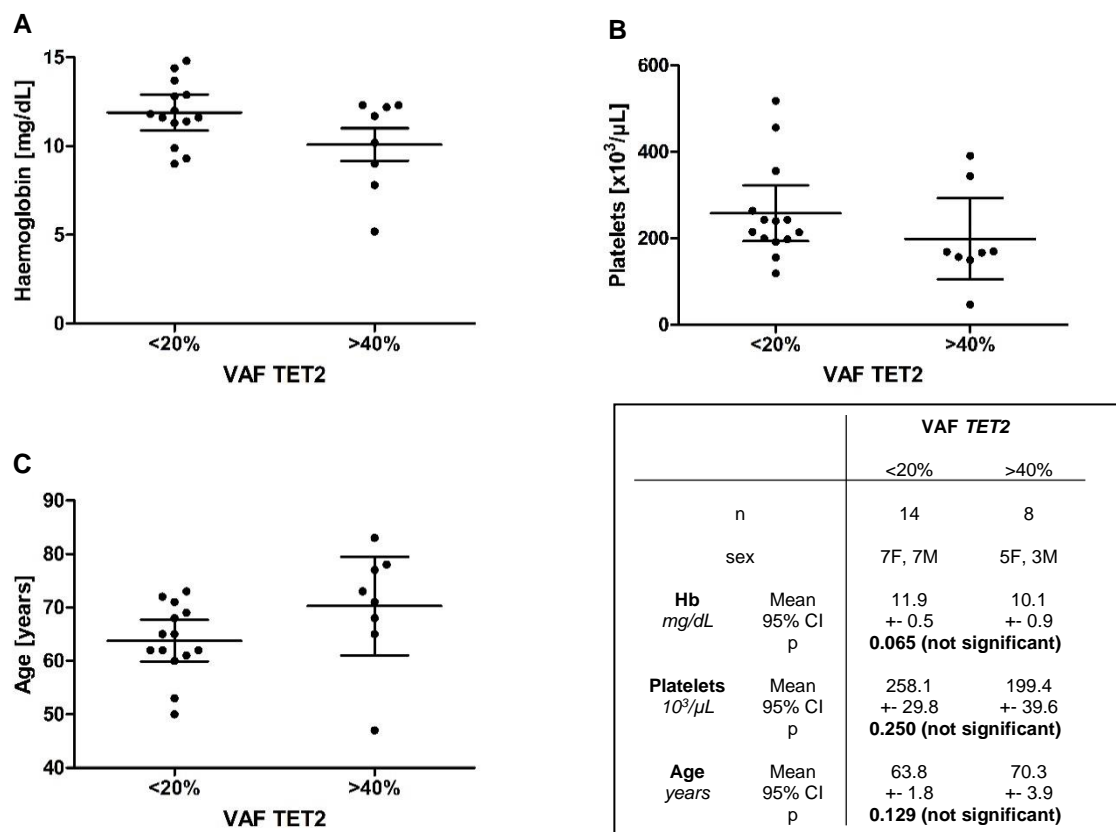


Figure 17 Comparison of blood parameters in subgroups with high and low *TET2* mutation frequencies. In this cohort, subgroups seemed to exist with either a high (>40%) or low (<20%) *TET2* VAF. Both subgroups were compared with each other concerning clinical parameters, including the haemoglobin (A) and platelet levels (B), as well as the age during blood extraction (C), which are all listed in the table above. In addition to that, the number of cases (n) of each subgroup, as well as the gender distribution into men (M) and women (F) are included. Furthermore, means and 95% confidence intervals (CI), as well as p values are presented.

3.5.2 Successive Molecular Analysis

NGS was conducted on bone marrow samples using a custom panel covering recurrently mutated genes in MDS. A detailed summary of the included genes is shown in the methods section (**Table 3**). No other mutations concerning *TET2* and *DNMT3A* were detected, which have not already been identified with the AITL panel. Therefore, only additional mutations of MDS related genes are shown in **Table 11**. NGS quality was comparable to previous experiments with the AITL panel in terms of average reads per amplicon, average amplicon reading end-to-end, as well as the uniformity of amplicon coverage. Throughout all experiments, no amplicon was remarked with less than 100 reads.

Overall, most cases did not reveal any further genetic variations in MDS related genes; however, one mutation existed within both biopsies of case G (*SF3B1*, VAF 41% and 43%). Moreover, relevant variants could be confirmed in cases L (*U2AF1*, VAF 3%), O (*SRSF2*, VAF 16%) and S (*TP53*, VAF 7%). These four cases altogether belonged to the subgroup with *TET2* VAF above 40%. Apart from that, NGS analysis was not possible with DNA of case A.

Table 11 Genetic findings in MDS genes. DNA from bone marrow of at least one sample per case was analysed with NGS concerning MDS relevant genes (red), including variant allelic frequency (VAF) and the VarSome (VS) prediction.

Case	Sample	TET2		DNMT3A		MDS Genes			
		Mutation	VAF	Mutation	VAF	Gene	Mutation	VAF	VS
A	A	c.2332C>T, p.Q778*	44%	-	-	n.d.	n.d.	n.d.	n.d.
B	B.1	c.3224A>G, p.D1075G c.4038delT, p.N1346fs	50% 1%	c.2645G>A, p.R882H	0.8%	-	-	-	-
C	C	c.3088C>T, p.Q1030*	46%	-	-	-	-	-	-
D	D	c.2754_2761del, p.R918fs	1%	-	-	-	-	-	-
E	E.1	c.5399_5400insT, M1800fs	5%	-	-	-	-	-	-
		c.4503_4504del, p.Q1501fs	2%						
F	F.1	c.3810_3817del, p.C.1271fs	18%	c.1755_1756insG, p.C586fs	10%	-	-	-	-
				c.2206C>T, p.R736C	3.3%				
G	G.1	c.3782G>C, p.R1261P	45%	c.1304_1305insT, p.Y436fs	43%	SF3B1	c.2098A>G, p.K700E	41%	P
	G.2	c.3782G>C, p.R1261P c.3893delG, p.C1298fs	46% 0.4%	c.1304_1305insT, p.Y436fs	38%	SF3B1	c.2098A>G, p.K700E	43%	P
H	H	c.4249G>T, p.V1417F	3.9%	c.2645G>A, p.R882H	3%	-	-	-	-
I	I	c.3812G>A, p.C1271Y	7%	c.976C>T, p.R326C	3%	-	-	-	-
J	J	-	-	c.976C>T, p.R326C c.2711C>T, p.P904L	18% 1.4%	-	-	-	-
K	K	c.3658_3677del, p.T1220fs	0.3%	-	-	-	-	-	-
L	L	c.840_841insT, p.N281*	44%	c.1296delC, p.Y432*	43%	U2AF1	c.470A>G, p.Q157R	3%	LP
		c.4854C>G, p.Y1618*	44%						
M	M	c.1720C>T, p.Q574*	0.9%	-	-	-	-	-	-
		c.5582G>A, p.G1861E	0.3%						
O	O	c.3796A>T, p.N1266Y	48%	c.1603_1604ins#, p.Y528_Q534dup	37%	SRSF2	c.284C>A, p.P95H	16%	P
		c.5650A>G, p.T1884A	44%						
P	P.1	c.3788G>A, p.C1263Y	3%	c.2645G>A, p.R882H	1.9%	-	-	-	-
	P.2	c.3788G>A, p.C1263Y	4%						
Q	Q	-	-	-	-	-	-	-	-
R	R	-	-	-	-	-	-	-	-
S	S	c.2759delT, p.L920*	32%	-	-	TP53	c.746G>C, p.R249T	7%	P
		c.5527_5530dup, p.D1844fs	44%						
T	T	-	-	-	-	-	-	-	-
U	U.1	c.2599T>C, p.Y867H	46%	c.912del, p.W305Gfs c.1443C>A, p.Y481* c.1031T>C, p.L344P	14% 8% 3%	-	-	-	-
		c.5680C>A, p.P1894T	16%						
		c.2919C>A, p.C973*	5%						
	U.2	c.2599T>C, p.Y867H c.5680C>A, p.P1894T c.2919C>A, p.C973*	50% 18% 10%	c.912del, p.W305Gfs c.1443C>A, p.Y481* c.1031T>C, p.L344P	19% 5% 1.6%	- - -	- - -	- - -	
V	V	c.2862G>A	14%	-	-	-	-	-	-
W	W	-	-	-	-	-	-	-	-

n.d. (not detectable)

#ACGACGACGACGGCTACCAGT (case O, DNMT3A)

VarSome (VS) prediction: pathogenic (P)
likely pathogenic (LP)
uncertain significance (US)
likely benign (LB)

4 Discussion

4.1 Patient Collective

4.1.1 Characteristics

The main question was whether the *TET2* and *DNMT3A* mutations identified in the lymph nodes infiltrated with AITL were also identified in the bone marrow biopsies with and without AITL infiltration to clarify whether these are CHIP mutations. In order to answer this question, we compared the genetic patterns of these lymph nodes in a total of 22 cases with corresponding biopsies of bone marrow. An initial aspect relied on the question, if the patient collective was biased by this criterion in terms of representativeness? The median age of the collective at AITL onset was 68 years (range of 47 – 83 years), which corresponds to that of published data. Studies from the first decade of the century mention a median age at onset ranging from 59 to 65 years (de Leval et al., 2010, Mourad et al., 2008). More recent studies from the National Cancer Database of the United States of America state an average age of 67 years (Ermann et al., 2019). In addition to that, the gender distribution in this study is well balanced with twelve females and ten males, which seems to be in line with literature. Although a slight predominance of males has been reported, it is still seen controversial due to the low prevalence of AITL (Dogan et al., 2017).

4.1.2 Sample Quality

Overall, only one sample (Q.2) from the initial cohort had to be excluded from further analysis due to lack of tissue. Although an amplifiable amount of DNA could have been extracted, a pathological assessment was not possible. Nevertheless, the large majority of FFPE bone marrow biopsies seem to be ideal to use for NGS experiments, because the decalcification is performed shortly with EDTA. All specimens date back from 2005 to 2017 and were fixated, archived, and processed similar. Different parameters are reported to impair the DNA quality in bone marrow biopsies, including thickness of tissue, formalin quality, decalcification procedures or conditions of storage (Srinivasan et al., 2002, Do and Dobrovic, 2015, Bettoni et al., 2017). Some biopsies revealed DNA integrities

of 200 base pairs or below; however, they were treated with a DNA repair kit prior to sequencing experiments. The quality of sequencing results was comparable to untreated samples of higher integrity in terms of NGS specific quality characteristics, including uniformity of amplicon coverage, amplicon reading end-to-end and average reads per amplicon. Taken together the results emphasize the feasibility of our protocol.

4.1.3 Bone Marrow Infiltration

In this cohort, 9/22 (41%) cases showed lymphoma involvement of the bone marrow specimen microscopically with positivity in TFH-specific markers by immunohistochemistry. In accordance with the literature, 45 – 70% of the patients with diagnosed AITL show bone marrow infiltration at the time of diagnosis (Cho et al., 2009, Lewis et al., 2020). The slight discrepancy might be explained by the timepoint of bone marrow extractions. Some biopsies were taken even months before the onset of AITL, for instance cases P and U. Overall, bone marrow samples of 15/22 (68%) cases were extracted before the date of AITL diagnosis. In 6/22 (27%), biopsies of even more than a month before the diagnosis exist. Moreover, AITL bone marrow involvement might be diagnostically challenging if infiltration occurs at an early stage. Neoplastic cells do not typically build characteristic lymphoma architecture as seen in affected lymph nodes (Gerlach et al., 2019). Therefore, additional analysis might be useful, for instance clonality analysis, if bone marrow infiltration patterns are rather diffuse with scattered neoplastic cells. Even though clonality analysis of bone marrow and corresponding lymph nodes are unable to replace a morphological assessment, it might be useful to identify early-stage infiltration (Gerlach et al., 2019).

4.2 Molecular Analysis

4.2.1 RHOA

RHOA^{G17V} is highly specific to AITL and present in most patients. In our cohort, this mutation was confirmed in 14/22 (63%) cases in positive lymph nodes. Also concerning this aspect, the patient collective seems to be unbiased, as data is in line with a reported prevalence of 50 – 70% (Sakata-Yanagimoto et al., 2014, Yoo et al., 2014). Regarding bone marrow specimens; however, only two cases of the collective carried *RHOA*^{G17V} and allelic frequencies were even below 2%. These genetic findings account for infiltrated neoplastic cells, as both samples showed clear lymphoma involvement microscopically. Apart from these two biopsies, the mutation was not found in any other bone marrow sample, which supports the idea of *RHOA*^{G17V} as a switch of malignant transformation (Yoo et al., 2014). Most probable, neoplastic precursor cells gain this mutation and subsequently progress into neoplastic cells outside of the bone marrow. In some cases; however, neoplastic cells re-enter the haematopoietic niche, which demonstrates lymphoma infiltration.

4.2.2 IDH2

IDH2^{R172} exists in 6/22 (27%) cases of the study collective, which corresponds a reported prevalence of 20 – 45% in AITL (Cairns et al., 2012, Sakata-Yanagimoto et al., 2014). Most interestingly, *IDH2*^{R172} and genetically altered *TET2* seem to coexist within AITL, which has been already shown in a previous project (Steinhilber et al., 2019). In consequence to that, one question in particular relied on the molecular patterns of this subgroup. In this study, all six cases carried the same *TET2* mutations in the bone marrow and the corresponding lymphoma specimen. In contrast to that; however, only one sample demonstrated *IDH2*^{R172} within bone marrow but also clear lymphoma infiltration microscopically.

4.2.3 *TET2* and *DNMT3A* mediated Clonal Haematopoiesis

Although *RHOA* was reported to be the most frequently mutated gene in AITL, recent studies have suggested *TET2* to be the most frequently altered gene. In this cohort, 19/22 (86%) cases carry at least one *TET2* mutation, which is in line with recent reports demonstrating *TET2* mutation rates of even 90 – 100% when NGS was used (Schwartz et al., 2017, Wang et al., 2017, Lewis et al., 2020). All patients with a genetic variation of *TET2* in the bone marrow carried the same mutation in the lymphoma specimen, which indicates clonal derivation of neoplastic cells from haematopoietic precursors. The mutation profiles of lymphoma tissue showed additional *TET2* mutations, which did not exist in bone marrow and most probable evolved in the course of the disease. Overall, genetic variations of *TET2* within bone marrow could even be found in 17/22 (77%) cases in this cohort, which by far exceeds the prevalence in healthy elderly individuals. Studies from peripheral bloods cells of healthy individuals older than 70 years showed somatic mutations in 9.5 – 18.4% of any genes commonly involved into haematopoietic malignancies, including *TET2*, *DNMT3A* and *ASXL1* (Jaiswal et al., 2014).

Apart from the high prevalence, *TET2* is also the gene with the highest mutation frequencies in our study collective. Except five cases, which did not carry corresponding mutations in lymphoma and bone marrow, altered *TET2* is the mutational finding with the highest VAF in each case. It is therefore most reasonable inactivation of *TET2* occurs at an early stage and seems to represent a key process in the development of AITL, which has been postulated previously by our group and others (Steinhilber et al., 2019, Lewis et al., 2020).

The impact of *TET2* loss-of-function mutations have already been reported abundantly concerning myeloid cancers, as genetic variations are associated with increased stem-cell renewal and haematopoietic defects (Delhommeau et al., 2009, Langemeijer et al., 2009, Moran-Crusio et al., 2011). Our data strongly supports the concept of *TET2* loss-of-function mutations leading to clonal haematopoiesis, which thereupon supports further acquisition of mutations like *RHOA*^{G17V} and *IDH2*^{R172} in the pathogenesis of AITL (Lewis et al., 2020). In addition to the high prevalence of *TET2* mutations in our study cohort, each

variant was unique and could not be identified in any other case. About two thirds of all mutations were directly located within functional domains probably causing functional loss. Mutations, which were located upstream of these domains, were mostly frameshift or nonsense mutations also probably impairing *TET2*'s natural function. Moreover, 9/17 (53%) cases carried even two or three different mutations implying high selection pressure for inactivation of *TET2*. Most interestingly, *TET2* mutations existed in *IDH2^{R172}* and/or *RHOA^{G17V}* subgroups significantly more often compared with *RHOA* wildtype subgroups. Except case J, 13/14 (93%) *IDH2^{R172}* and *RHOA^{G17V}* positive cases carried mutated *TET2* in the bone marrow and neoplastic cells. Although case J revealed mutated *TET2* within lymphoma tissue, the mutation was not present in DNA from the bone marrow.

Genetically altered *DNMT3A* seems to contribute to AITL tumorigenesis as well, but rather complementary to *TET2* mutations. Although the prevalence of mutated *DNMT3A* within AITL is higher, compared with healthy elderly, it is less frequent than *TET2* (Jaiswal et al., 2014). In this study, 10/22 (45%) cases revealed alterations concerning this gene, which is above a reported prevalence of 20 – 30% in AITL (Sakata-Yanagimoto et al., 2014, Palomero et al., 2014, Dobay et al., 2017). There was almost a complete agreement of *DNMT3A* mutations in the bone marrow and lymph nodes, as corresponding mutation profiles existed in 9/10 (90%) cases. All *DNMT3A* mutations were either within functional domains or nonsense mutations probably leading to functional loss.

Concerning the prevalence and the VAF, *TET2* mutations predominated in our study collective. Interestingly, mutations of both epigenetic regulators showed oncogenic cooperation. All *IDH2^{R172}* and/or *RHOA^{G17V}* cases revealed at least one mutation within one of the two epigenetic regulators with a major impact of *TET2* mutations. Recent studies emphasise the concept of clonal haematopoiesis within AITL as a consequence of double mutated, *TET2* and *DNMT3A*, precursor cells. In our study series, 8/22 (36%) cases showed a double mutated genetic profile perfectly fitting to the reported prevalence of 32% (Lewis et al., 2020).

4.2.4 Germline Variants

Various bone marrow samples exhibited high VAF of 44 – 50% in *TET2* or *DNMT3A* in our study cohort suggesting them as SNPs or possible heterozygous germline mutations. We have, therefore, reviewed these variants initially with open source online tools (Cosmic, Exome Variant Server), which allowed us to rule them out as rare SNPs and predict them as damaging mutations. We have subsequently looked up for possible germline variants in these cases.

Although no germline component has been described in AITL so far, genetic predisposition exists for genes in other haematopoietic malignancies (Furutani and Shimamura, 2017). For instance, various leukaemia and lymphoma subtypes are associated with the Li-Fraumeni syndrome. Due to a germline mutation in *TP53*, patients have a tremendously higher risk to develop any subtype of cancer. Also haematopoietic neoplasms are described with the Li-Fraumeni syndrome, only 4% of cancers account for them, as most frequent entities are breast cancer and malignancies of the soft tissue (Guha and Malkin, 2017). Apart from the Li-Fraumeni syndrome, familiar clustering of MDS and AML has been reported in consequence to germline mutations. Although, MDS and AML are typically sporadic late-onset malignancies, a variety of genes have been identified being involved into hereditary, early-onset myelodysplastic syndromes, for instance *RUNX1* (Bannon and DiNardo, 2016).

As germline variants occur early during zygote development or even before fertilization, all cells within the organism carry this genetic setup. We have conducted NGS on DNA extracted from nonhematopoietic gastrointestinal tissue of three representative cases to identify possible germline variants in our cohort. The same mutations were found; however, VAF ranged from 4 – 8%, which rules out the existence of *TET2* or *DNMT3A* germline predisposition. Nevertheless, some cells obviously carry the same mutational profile, which might be explained by scattered haematopoietic cells with CHIP in the biopsy. A large proportion of hematopoietic cells in bone marrow seemed to carry these mutations due to high VAF. It is therefore most reasonable that other peripheral cells of haematopoietic descent, including subgroups of leukocytes, carried the same mutations.

4.3 Examination of MDS Properties

4.3.1 Blood Counts

In addition to molecular analysis, a correlation of clinical parameters with mutation frequencies in *TET2* was conducted to examine, whether high VAF is affecting blood levels as an indicator of notable clonal haematopoiesis or even coexisting MDS (Hirsch et al., 2018). Initial blood counts of hospitalisation were used to avoid bias concerning possible applications of blood products during the stay. Although a trend of increased VAF and reduced Hb and platelet values could be seen, a linear regression was not observed, as indicated by low R^2 values, which was most probable secondary to the small sample size and the irregular distribution. Two subgroups existed within this study collective concerning the VAF in *TET2*. While 8/22 (36%) cases revealed genetic alterations of *TET2* in bone marrow with a VAF of more than 40%, the other bone marrow cases were either wildtype or showed VAF below 20%. No single biopsy within this cohort carried altered *TET2* between 20 – 40% in the bone marrow, thus we decided to compare these two subgroups (*TET2* <20% vs. >40%) concerning clinical parameters, including platelet counts and Hb values.

The subgroup with high VAF in *TET2* revealed an average Hb of 10.1 g/dL, which corresponds to a moderate anaemia according to the WHO (Organization, 2011). The average platelet count with $199 \times 10^3/\mu\text{L}$ was reduced, but still in the reference range. The subgroup with wildtype or low VAF in *TET2* shows an average Hb of 11.9 g/dL indicating a mild anaemia and an average platelet count of $258 \times 10^3/\mu\text{L}$. Although blood parameters were reduced in the subgroup with high VAF, differences were not statistically significant. At least a trend could be seen, which fits the genetic profile and clinical presentation of progressed clonal haematopoiesis and MDS (Steensma et al., 2015, Li et al., 2016, Sperling et al., 2017).

4.3.2 Genetic Analysis

TET2 is not only one of the most frequently mutated genes in AITL, but also in myeloid malignancies, such as MDS. With a prevalence of 30 – 35% in all MDS

patients, genetically altered *TET2* is the most frequently mutated gene (Haferlach et al., 2014). Interestingly, 8/22 (36%) cases revealed genetic alterations of *TET2* in bone marrow with a VAF of more than 40%. Mutations with such a high VAF are suspicious for coexisting MDS, thus we decided to conduct further analysis concerning MDS relevant genes (Hirsch et al., 2018). Hereby, a subgroup of 4/22 (18%) cases showed additional genetic findings, while none of the subgroup with a VAF below 20% revealed further genetic abnormalities.

Case G is the only of the four cases, which showed a comparable VAF in *SF3B1* as seen in *TET2*. Cases L (*U2AF1*, 3%), O (*SRSF2*, 16%) and S (*TP53*, 7%) carried MDS relevant mutations; however, frequencies were far less compared with *TET2*. After identifying the high allelic frequencies in *TET2*, we have looked up for already existing MDS diagnosis in the collective. G was the only case of the cohort with an already diagnosed MDS in its medical history. This case revealed a progressed stage of MDS, which was not only supported by high VAF in mutated *TET2*, *DNMT3A* and *SF3B1*, but also demonstrated by the severe anaemia as seen in the blood count (Steensma et al., 2015, Sperling et al., 2017).

Cases L, O and S were suspicious for coexisting MDS, but biopsies need to be re-evaluated. Case O and L carried high VAF in both, *TET2* and *DNMT3A* mutations, which had been recently demonstrated to promote myelodysplastic changes (Lewis et al., 2020). Furthermore, cases L and S revealed suspicious findings within the blood counts. Both cases showed reduced platelet levels and case S even moderate anaemia, which might be explained by progressed MDS (Steensma et al., 2015, Li et al., 2016, Sperling et al., 2017).

Most likely, the three undiagnosed cases demonstrate beginning onset of MDS, while case G reveals the disease in a progressed stage, in contrast. Concerning the age at onset, biopsies of case L (83 years) and S (73 years) fit with a reported median age at MDS diagnosis of 71 – 76 years (Sperling et al., 2017). Only case O (65 years) is rather young to reflect consequences of beginning MDS; however, *TET2* is highly mutated and *SRSF2* is altered as well. The coexistence of both mutated genes might explain the early onset, as *TET2* mutations positively correlate with genetic alterations of *SRSF2* in MDS (Haferlach et al., 2014).

4.3.3 Divergent Evolution of AITL and MDS

Clonal Haematopoiesis has been postulated as a precursor lesion for different haematopoietic malignancies, including AITL, as well as MDS (Papaemmanuil et al., 2013, Jaiswal et al., 2014). Both entities not only share common clinical characteristics, i.e. pancytopenia, but also overlapping genetic profiles including *TET2* and *DNMT3A*. In our study, one case already has confirmed MDS as secondary diagnosis and even three more cases possess a suspicious genetic and clinical presentation. Our data suggests the coevolution of both entities from common precursors, at least in a subgroup of cases, which is in line with latest reports. Several studies showed correlations of myeloproliferative and lymphoproliferative malignancies just recently (Holst et al., 2019, Lewis et al., 2020). Pluripotent stem/progenitor cells acquire genetic hits within *TET2* with subsequent clonal expansion. In the following, further mutations are gained, favourably *DNMT3A*, which supports clonal haematopoiesis. Changes within precursor cells significantly increase the risk of malignant progression, either into MDS, or into AITL depending on the genetic profile (**Figure 18**).

Just recently, a study showed this divergent evolution of MDS and AITL from *TET2* and *DNMT3A* double-mutated haematopoietic stem/progenitor cells. Four of 22 (18%) cases with diagnosed AITL and mutations within both epigenetic regulators developed myeloid neoplasms in the course of the disease (Lewis et al., 2020). In consequence to that, the clinical situation for patients with AITL not only aggravates, but also the risk for developing further comorbidities is increased. Recent data emphasise an increased prevalence of myelodysplastic changes in patients with AITL compared with the general population and especially the risk is also higher in the subsequent development of AML (Kommalapati et al., 2019).

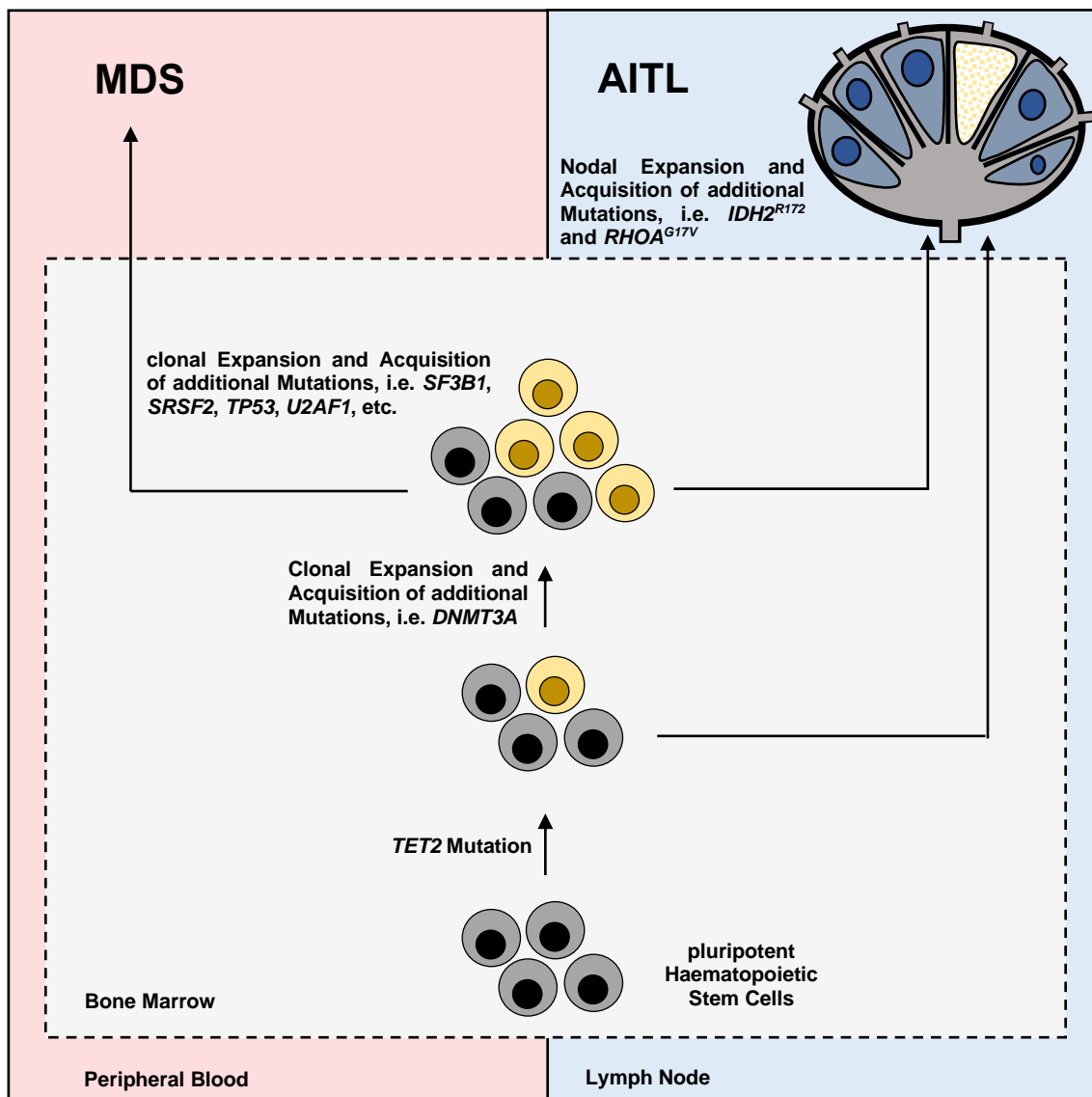


Figure 18 Divergent evolution of MDS and AITL as consequence of clonal haematopoiesis. Pluripotent haematopoietic stem cells within bone marrow acquire mutations resulting in clonal haematopoiesis. In both entities, *TET2* mutations (yellow) represent early events with subsequent clonal expansion and possible acquisition of additional genetic hits, i.e. *DNMT3A*. Upon that, dysregulated progenitor cells progress with the divergent development of AITL or MDS, depending on the mutational profile. While clonal progenitors emigrate from bone marrow and progress into AITL within lymph nodes, MDS remain in the haematopoietic compartment with the potential to progress into AML. Interestingly, AITL and MDS coexists in a subgroup of cases in consequence of a common mutated progenitor.

4.4 Conclusion

The main goal of this project was to analyse the mutational dynamics between the four most frequently mutated genes in AITL. Bone marrow samples were retrieved and compared with corresponding lymphoma specimens concerning mutational profiles. Although the availability of bone marrow biopsies was a possible source of bias in this retrospective study, the collective is appropriate in various patient characteristics, such as age at onset and gender balance, as well as the genetic profile of lymphoma tissue. Moreover, bone marrow biopsies decalcified with EDTA seem to be ideal for NGS experiments of patients with AITL, as they are not only commonly gained during clinical routine, but also represent an appropriate source of haematopoietic tissue with amplifiable DNA.

In our study, multiple findings support the hypothesis of clonal haematopoiesis in patients with AITL with a major impact of altered *TET2*. Loss-of-function mutations of this gene are present in most cases, reveal high VAFs of up to 50%, and often carry two or more mutations indicating that there is a strong pressure to inactivate *TET2* in the development of this disease. Furthermore, our data support the role of *DNMT3A* to be involved in clonal haematopoiesis, especially, if mutations exist in addition to *TET2*, as seen in about a third of the collective. The inactivation of either of these two epigenetic regulators represents early events in haematopoietic precursors promoting the acquisition of further genetic hits, such as *RHOA*^{G17V} and *IDH2*^{R172}. Interestingly, exceptionally high VAF in *TET2* or *DNMT3A* were detected in about a third of all patients. To exclude germline variants as a possible reason, we analysed DNA of non-hematopoietic tissue in three cases, in which biopsies were available and demonstrated that there are no germline mutations. Further analysis of clinical parameters, such as Hb and platelet counts, as well as additional sequencing experiments raised the possibility of a coexisting MDS, which will be in the focus of upcoming research projects. Although the results of this project contribute to better understand the lymphomagenesis in AITL, some questions will remain unsolved and need to be addressed in subsequent experiments.

4.5 Outlook

Overall, the results of this project provide further insights into the role of haematopoietic clonality for the development of AITL. Nonetheless, some aspects need to be addressed in upcoming studies, starting with additional genetic analysis. We were not able to identify mutations in all cases of this study collective. In subgroup 3, three cases do not show any genetic alteration in any of the four most frequently mutated genes, neither in bone marrow, nor in lymph nodes. Further sequencing experiments will be conducted on genes, which had not been covered with the AITL or MDS panel so far. Amongst them are genes of the TCR signalling pathway, which are occasionally altered in AITL, including *PLCγ*, *CD28*, *FYN* and *VAV1* (Vallois et al., 2016, Fukumoto et al., 2018). Apart from excessive sequencing experiments, clonality analysis is intended as well. So far, we have matched DNA of lymphoma specimens with bone marrow regarding corresponding AITL mutation patterns. We were able to detect most lymphoma mutations within haematopoietic precursors; however, infiltration was only detectable in about 41% of all cases. *TCR* clonality analysis is a very powerful tool because knowing the specific sequence of the T-cell clone in lymph node, we can identify small clones in the bone marrow even without clear evidence of histological infiltration.

In addition, the connection of AITL and MDS will be the focus of future projects. Our data strongly suggests a linkage of both entities at least for a subgroup of cases, with *TET2/DNMT3A* mutations as a genetic linker (Lewis et al., 2020). Hereby, we intend not only to conduct further sequencing experiments, but also a profound assessment including more clinical parameters. Moreover, a repeated pathological evaluation of all cases will be conducted concerning MDS.

5 Summary

5.1 Summary (English)

Angioimmunoblastic T-cell lymphoma (AITL) is one of the most frequent mature T- and NK-cell neoplasms and characterised by a severe clinical presentation. Its genetic profile has been intensively studied in the past years, not only for diagnostic purposes, but also for a better understanding of this disease. AITL harbours a characteristic mutational landscape including *RHOA*^{G17V} and *IDH2*^{R172}, as well as variations of *DNMT3A* and *TET2*. As the roles of genetically altered *TET2* and *DNMT3A* are not fully understood in AITL so far, we have tried to examine the dynamics between the different genes, especially concerning clonal haematopoiesis of indeterminate potential (CHIP). Therefore, we matched mutation profiles of AITL infiltrated lymph nodes with corresponding bone marrow samples of 22 cases.

A histopathological evaluation, as well as an examination of DNA integrity via PCR was conducted. Only one specimen had been excluded from further analysis due to low DNA quality. Amplifiable DNA could have been extracted from 29 bone marrow biopsies from a total of 22 cases, which were subsequently sequenced and compared with genetic patterns found in lymph nodes. The study collective was representative in several aspects, for instance the age at onset, gender distribution, as well as the mutation patterns are in line with the literature. While *RHOA*^{G17V} was present in 63% and *IDH2*^{R172} in 27% of all lymph node biopsies, mutations could not be detected in bone marrow samples except for two cases with clear morphological lymphoma infiltration. Moreover, 41% of all cases carried *DNMT3A* mutations in the lymph node and in corresponding bone marrow samples. In 86% of all cases, *TET2* mutations were present in the lymph node and bone marrow biopsies except for two cases. Interestingly, each *TET2* mutation was unique, the majority of cases showed at least two different mutations and variant allelic frequencies were always higher compared to mutations of *DNMT3A*, *RHOA* or *IDH2*. Altogether, our data indicate that there is a strong pressure to inactivate *TET2* during AITL lymphomagenesis. Importantly, the subgroup of cases with both, *IDH2* and/or *RHOA* mutations in lymph node

biopsies, almost always, carried *TET2* mutations in the bone marrow. Therefore, this study demonstrates that *TET2* mutations occur before the development of AITL, and other mutations, and suggest that the inactivation of *TET2* might be necessary for the development of AITL. This finding underscores the concept of clonal haematopoiesis with indeterminate potential and shows importance of CHIP as a precursor lesion for the development of AITL.

As *TET2* and *DNMT3A* mutations were high in eight cases with variant allelic frequencies of 44 – 50%, subsequent molecular and clinical assessment were conducted. DNA from non-haematopoietic tissue was extracted, sequenced and matched with the mutation profiles from three cases to exclude germline variants as a possible reason for the high allelic frequencies. This subgroup of eight cases showed reduced level of haemoglobin and platelet counts, although the difference was not statistically significant, further analysis concerning relevant genes in myelodysplastic syndrome (MDS) were performed. In four of these eight cases additional mutations could have been detected in *SF3B1*, *SRSF2*, *TP53* and *U2AF1*, which altogether further demonstrate the association between MDS and AITL in this cohort. Genetically altered *TET2* and *DNMT3A* seem to promote clonal haematopoiesis, which again favours accumulation of further mutations and supports tumorigenesis. The association between these two haematopoietic malignancies, AITL and MDS, will be subject of further projects.

5.2 Zusammenfassung (Deutsch)

Das angioimmunoblastische T-Zell-Lymphom (AITL) gehört zu den häufigsten reifen T- und NK-Zell Neoplasien und zeichnet sich durch einen schwerwiegenden klinischen Verlauf aus. In den vergangenen Jahren wurden Erkenntnisse über das genetische Profil gewonnen, die nicht nur der Diagnostik dienen, sondern vor allem auch Einblicke in die Krankheitsentstehung bieten. Hierzu zählen insbesondere Mutationen um *RHOA*^{G17V} und *IDH2*^{R172}, aber zuletzt vor allem auch in *TET2* und *DNMT3A*. Da die Rolle von *TET2* und *DNMT3A* bei AITL weitestgehend ungeklärt ist, versuchten wir mit dieser Studie die Dynamik im Mutationsgeschehen zwischen den verschiedenen Genen zu untersuchen, insbesondere hinsichtlich des Vorliegens einer klonalen Hämatopoese unklarer Signifikanz (CHIP). Hierbei haben wir Mutationsprofile von Lymphomgewebe aus Lymphknoten mit korrespondierenden Knochenmarkbiopsien von insgesamt 22 diagnostizierten AITL Fällen verglichen.

Alle Fälle wurden histopathologisch evaluiert und die DNA-Integrität mittels PCR überprüft. Lediglich eine Probe wurde aufgrund mangelhafter Qualität zu Beginn der Studie ausgeschlossen. Amplifizierbare DNA konnte aus 29 Knochenmarkproben von insgesamt 22 Fällen isoliert, sequenziert und mit dem Mutationsmuster der Lymphknoten verglichen werden. Es zeigte sich, dass das Patientenkollektiv hinsichtlich vieler Merkmale repräsentativ ist, beispielsweise entsprechen das Erkrankungsalter, die Geschlechterverteilung, sowie die Mutationsprofile den Referenzwerten in der Literatur. Während *RHOA*^{G17V} in 63% und *IDH2*^{R172} in 27% der Fälle im Lymphknoten nachgewiesen konnten, waren diese beiden Mutationen lediglich im Knochenmark von zwei Fällen mit ausgeprägter morphologischer Lymphominfiltration detektierbar. Davon abgesehen zeigten sich in 41% der Fälle Mutationen in *DNMT3A* in Lymphknoten und im korrespondierenden Knochenmark. In 86% der Fälle zeigten sich Veränderungen von *TET2* im Lymphknoten und bis auf zwei Fälle auch in den Knochenmarkproben. Interessanterweise war jede *TET2* Mutation individuell, es zeigten sich mehrheitlich mindestens zwei Mutationen und die detektierte Allelfrequenz waren stets höher als Mutationen in *DNMT3A*, *RHOA* oder *IDH2*. In der Gesamtschau sprechen unsere Daten für einen hohen Mutationsdruck

hinsichtlich *TET2* bei der Entwicklung von AITL. Interessanterweise existieren in der Untergruppe von Fällen, die sowohl *RHOA*^{G17V} als auch *IDH2*^{R172} im Lymphom aufwiesen, nahezu komplett *TET2* Mutationen im Knochenmark. Deshalb zeigt unsere Untersuchung, dass *TET2* bereits vor AITL Entstehung und vor weiteren Genen mutiert und lässt vermuten, dass die Inaktivierung von *TET2* für die Entstehung von AITL notwendig ist. Diese Erkenntnis untermauert das Konzept einer klonalen Hämatopoese unklarer Signifikanz und deutet auf die Wichtigkeit von CHIP als Vorläuferläsion bei der Entstehung von AITL.

Nachdem *TET2* und *DNMT3A* Mutationen in acht Fällen Frequenzen von 44 – 50% aufwiesen, wurden weitere molekulargenetische Untersuchungen vollzogen und klinische Parameter bestimmt. An drei Fällen wurde beispielhaft DNA aus nicht-hämatopoetischem Gewebe isoliert und sequenziert, um Keimbahnvarianten auszuschließen. Da diese Untergruppe von acht Fällen eine ausgeprägtere, wenn auch nicht signifikant niedrigere, Hämoglobin- und reduzierte Thrombozytenzahl zeigte, wurde eine genetische Untersuchung auf relevante Gene des myelodysplastischen Syndroms (MDS) veranlasst. Bei vier der acht Fälle zeigten sich auf Knochenmarksebene weitere Mutationen in den Genen *SF3B1*, *SRSF2*, *TP53* und *U2AF1*, was in der Gesamtschau für einen engen Zusammenhang zwischen AITL und MDS für eine Untergruppe des Kollektivs spricht. Mutationen in *TET2* und *DNMT3A* scheinen eine klonale Hämatopoese zu begünstigen, auf Basis derer weitere Mutationen akkumulieren und sich bevorzugt Erkrankungen wie AITL und MDS ausbilden können. Weitere Studien werden folgen, bei der insbesondere dieser Zusammenhang der beiden Erkrankungen im Fokus stehen wird.

6 References

- ADES, L., ITZYKSON, R. & FENAUX, P. 2014. Myelodysplastic syndromes. *Lancet*, 383, 2239-52.
- ARBER, D. A., ORAZI, A., HASSERJIAN, R., THIELE, J., BOROWITZ, M. J., LE BEAU, M. M., BLOOMFIELD, C. D., CAZZOLA, M. & VARDIMAN, J. W. 2016. The 2016 revision to the World Health Organization classification of myeloid neoplasms and acute leukemia. *Blood*, 127, 2391-2405.
- ATTYGALLE, A. D., KYRIAKOU, C., DUPUIS, J., GROGG, K. L., DISS, T. C., WOTHERSPOON, A. C., CHUANG, S. S., CABECADAS, J., ISAACSON, P. G., DU, M. Q., GAULARD, P. & DOGAN, A. 2007. Histologic evolution of angioimmunoblastic T-cell lymphoma in consecutive biopsies: clinical correlation and insights into natural history and disease progression. *Am J Surg Pathol*, 31, 1077-88.
- BANNON, S. A. & DINARDO, C. D. 2016. Hereditary Predispositions to Myelodysplastic Syndrome. *Int J Mol Sci*, 17.
- BASHA, B. M., BRYANT, S. C., RECH, K. L., FELDMAN, A. L., VRANA, J. A., SHI, M., REED, K. A. & KING, R. L. 2019. Application of a 5 Marker Panel to the Routine Diagnosis of Peripheral T-Cell Lymphoma With T-Follicular Helper Phenotype. *The American journal of surgical pathology*, 43, 1282-1290.
- BETTONI, F., KOYAMA, F. C., DE AVELAR CARPINETTI, P., GALANTE, P. A. F., CAMARGO, A. A. & ASPRINO, P. F. 2017. A straightforward assay to evaluate DNA integrity and optimize next-generation sequencing for clinical diagnosis in oncology. *Exp Mol Pathol*, 103, 294-299.
- BRAY, F., FERLAY, J., SOERJOMATARAM, I., SIEGEL, R. L., TORRE, L. & JEMAL, A. 2018. GLOBOCAN estimates of incidence and mortality worldwide for 36 cancers in 185 countries. *Ca Cancer J Clin*, 68, 394-424.
- CAIRNS, R. A., IQBAL, J., LEMONNIER, F., KUCUK, C., DE LEVAL, L., JAIS, J. P., PARRENS, M., MARTIN, A., XERRI, L., BROUSSET, P., CHAN, L. C., CHAN, W. C., GAULARD, P. & MAK, T. W. 2012. IDH2 mutations are frequent in angioimmunoblastic T-cell lymphoma. *Blood*, 119, 1901-3.
- CHALLEN, G. A., SUN, D., JEONG, M., LUO, M., JELINEK, J., BERG, J. S., BOCK, C., VASANTHAKUMAR, A., GU, H., XI, Y., LIANG, S., LU, Y., DARLINGTON, G. J., MEISSNER, A., ISSA, J. P., GODLEY, L. A., LI, W. & GOODELL, M. A. 2011. Dnmt3a is essential for hematopoietic stem cell differentiation. *Nat Genet*, 44, 23-31.
- CHIHARA, D., ITO, H., MATSUDA, T., SHIBATA, A., KATSUMI, A., NAKAMURA, S., TOMOTAKA, S., MORTON, L. M., WEISENBURGER, D. D. &

- MATSUO, K. 2014. Differences in incidence and trends of haematological malignancies in Japan and the United States. *Br J Haematol*, 164, 536-45.
- CHO, Y. U., CHI, H. S., PARK, C. J., JANG, S., SEO, E. J. & HUH, J. 2009. Distinct features of angioimmunoblastic T-cell lymphoma with bone marrow involvement. *Am J Clin Pathol*, 131, 640-6.
- COHEN, A. L., HOLMEN, S. L. & COLMAN, H. 2013. IDH1 and IDH2 mutations in gliomas. *Curr Neurol Neurosci Rep*, 13, 345.
- COURONNE, L., BASTARD, C. & BERNARD, O. A. 2012. TET2 and DNMT3A mutations in human T-cell lymphoma. *N Engl J Med*, 366, 95-6.
- CROTTY, S. 2011. Follicular helper CD4 T cells (TFH). *Annu Rev Immunol*, 29, 621-63.
- DE LEVAL, L., GISSELBRECHT, C. & GAULARD, P. 2010. Advances in the understanding and management of angioimmunoblastic T-cell lymphoma. *Br J Haematol*, 148, 673-89.
- DE LEVAL, L., PARRENS, M., LE BRAS, F., JAIS, J. P., FATACCIOLI, V., MARTIN, A., LAMANT, L., DELARUE, R., BERGER, F., ARBION, F., BOSSARD, C., COPIN, M. C., CANIONI, D., CHARLOTTE, F., DAMAJ, G., DARTIGUES, P., FABIANI, B., LEDOUX-PILON, A., MONTAGNE, K., MOLINA, T., PATEY, M., TAS, P., PEOCH, M., PETIT, B., PETRELLA, T., PICQUENOT, J. M., ROUSSET, T., ROUSSELET, M. C., SOUBEYRAN, I., THIEBAULT, S., TOURNILHAC, O., XERRI, L., GISSELBRECHT, C., HAIOUN, C., DELSOL, G. & GAULARD, P. 2015. Angioimmunoblastic T-cell lymphoma is the most common T-cell lymphoma in two distinct French information data sets. *Haematologica*, 100, e361-4.
- DE LEVAL, L., RICKMAN, D. S., THIELEN, C., REYNIES, A., HUANG, Y. L., DELSOL, G., LAMANT, L., LEROY, K., BRIERE, J., MOLINA, T., BERGER, F., GISSELBRECHT, C., XERRI, L. & GAULARD, P. 2007. The gene expression profile of nodal peripheral T-cell lymphoma demonstrates a molecular link between angioimmunoblastic T-cell lymphoma (AITL) and follicular helper T (TFH) cells. *Blood*, 109, 4952-63.
- DELHOMMEAU, F., DUPONT, S., DELLA VALLE, V., JAMES, C., TRANNOY, S., MASSE, A., KOSMIDER, O., LE COUEDIC, J. P., ROBERT, F., ALBERDI, A., LECLUSE, Y., PLO, I., DREYFUS, F. J., MARZAC, C., CASADEVALL, N., LACOMBE, C., ROMANA, S. P., DESSEN, P., SOULIER, J., VIGUIE, F., FONTENAY, M., VAINCHENKER, W. & BERNARD, O. A. 2009. Mutation in TET2 in myeloid cancers. *N Engl J Med*, 360, 2289-301.
- DO, H. & DOBROVIC, A. 2015. Sequence artifacts in DNA from formalin-fixed tissues: causes and strategies for minimization. *Clin Chem*, 61, 64-71.

- DOBAY, M. P., LEMONNIER, F., MISSIAGLIA, E., BASTARD, C., VALLOIS, D., JAIS, J. P., SCOURZIC, L., DUPUY, A., FATACCIOLI, V., PUJALS, A., PARRENS, M., LE BRAS, F., ROUSSET, T., PICQUENOT, J. M., MARTIN, N., HAIOUN, C., DELARUE, R., BERNARD, O. A., DELORENZI, M., DE LEVAL, L. & GAULARD, P. 2017. Integrative clinicopathological and molecular analyses of angioimmunoblastic T-cell lymphoma and other nodal lymphomas of follicular helper T-cell origin. *Haematologica*, 102, e148-e151.
- DOGAN, A., GAULARD, P., JAFFE, E., MULLER-HERMELINK, H. & DE LEVAL, L. 2017. Angioimmunoblastic T-cell lymphoma and other nodal lymphomas of T follicular helper cell origin. *WHO classification of tumours of haematopoietic and lymphoid tissues*, 407-412.
- DUPUIS, J., BOYE, K., MARTIN, N., COPIE-BERGMAN, C., PLONQUET, A., FABIANI, B., BAGLIN, A.-C., HAIOUN, C., DELFAU-LARUE, M.-H. & GAULARD, P. 2006. Expression of CXCL13 by neoplastic cells in angioimmunoblastic T-cell lymphoma (AITL): a new diagnostic marker providing evidence that AITL derives from follicular helper T cells. *The American journal of surgical pathology*, 30, 490-494.
- ERMANN, D. A., VARDELL, V. A. & SILBERSTEIN, P. T. 2019. Angioimmunoblastic T-Cell Lymphoma: Patient Characteristics and Survival Outcomes. American Society of Hematology Washington, DC.
- FEDERICO, M., RUDIGER, T., BELLEI, M., NATHWANI, B. N., LUMINARI, S., COIFFIER, B., HARRIS, N. L., JAFFE, E. S., PILERI, S. A. & SAVAGE, K. J. 2013. Clinicopathologic characteristics of angioimmunoblastic T-cell lymphoma: analysis of the international peripheral T-cell lymphoma project. *Journal of Clinical Oncology*, 31, 240.
- FIGUEROA, M. E., ABDEL-WAHAB, O., LU, C., WARD, P. S., PATEL, J., SHIH, A., LI, Y., BHAGWAT, N., VASANTHAKUMAR, A., FERNANDEZ, H. F., TALLMAN, M. S., SUN, Z., WOLNIAK, K., PEETERS, J. K., LIU, W., CHOE, S. E., FANTIN, V. R., PAIETTA, E., LOWENBERG, B., LICHT, J. D., GODLEY, L. A., DELWEL, R., VALK, P. J., THOMPSON, C. B., LEVINE, R. L. & MELNICK, A. 2010. Leukemic IDH1 and IDH2 mutations result in a hypermethylation phenotype, disrupt TET2 function, and impair hematopoietic differentiation. *Cancer Cell*, 18, 553-67.
- FRIZZERA, G., MORAN, E. M. & RAPPAPORT, H. 1974. Angio-immunoblastic lymphadenopathy with dysproteinaemia. *Lancet*, 1, 1070-3.
- FUJISAWA, M., SAKATA-YANAGIMOTO, M., NISHIZAWA, S., KOMORI, D., GERSHON, P., KIRYU, M., TANZIMA, S., FUKUMOTO, K., ENAMI, T., MURATANI, M., YOSHIDA, K., OGAWA, S., MATSUE, K., NAKAMURA, N., TAKEUCHI, K., IZUTSU, K., FUJIMOTO, K., TESHIMA, T., MIYOSHI, H., GAULARD, P., OHSHIMA, K. & CHIBA, S. 2018. Activation of RHOA-

- VAV1 signaling in angioimmunoblastic T-cell lymphoma. *Leukemia*, 32, 694-702.
- FUKUMOTO, K., NGUYEN, T. B., CHIBA, S. & SAKATA-YANAGIMOTO, M. 2018. Review of the biologic and clinical significance of genetic mutations in angioimmunoblastic T-cell lymphoma. *Cancer Sci*, 109, 490-496.
- FURUTANI, E. & SHIMAMURA, A. 2017. Germline Genetic Predisposition to Hematologic Malignancy. *J Clin Oncol*, 35, 1018-1028.
- GERLACH, M. M., JUSKEVICIUS, D., VELA, V., DIRNHOFER, S. & TZANKOV, A. 2019. Bone Marrow Infiltration of Angioimmunoblastic T-Cell Lymphoma: Identification and Prognostic Impact of Histologic Patterns and Diagnostic Application of Ancillary Phenotypic and Molecular Analyses. *Archives of Pathology & Laboratory Medicine*.
- GUHA, T. & MALKIN, D. 2017. Inherited TP53 mutations and the Li-Fraumeni syndrome. *Cold Spring Harbor perspectives in medicine*, 7, a026187.
- HAFERLACH, T., NAGATA, Y., GROSSMANN, V., OKUNO, Y., BACHER, U., NAGAE, G., SCHNITTGER, S., SANADA, M., KON, A. & ALPERMANN, T. 2014. Landscape of genetic lesions in 944 patients with myelodysplastic syndromes. *Leukemia*, 28, 241-247.
- HIRSCH, C. M., NAZHA, A., KNEEN, K., ABAZEED, M. E., MEGGENDORFER, M., PRZYCHODZEN, B. P., NADARAJAH, N., ADEMA, V., NAGATA, Y., GOYAL, A., AWADA, H., ASAD, M. F., VISCONTE, V., GUAN, Y., SEKERES, M. A., OLINSKI, R., JHA, B. K., LAFRAMBOISE, T., RADIVOYEVITCH, T., HAFERLACH, T. & MACIEJEWSKI, J. P. 2018. Consequences of mutant TET2 on clonality and subclonal hierarchy. *Leukemia*, 32, 1751-1761.
- HOLST, J. M., PLESNER, T. L., PEDERSEN, M. B., FREDERIKSEN, H., MOLLER, M. B., CLAUSEN, M. R., HANSEN, M. C., HAMILTON-DUTOIT, S. J., NORGAARD, P., JOHANSEN, P., EBERLEIN, T. R., MORTENSEN, B. K., MATHIASSEN, G., OVLISEN, A., WANG, R., WANG, C., ZHANG, W., OMMEN, H. B., STENTOFT, J., LUDVIGSEN, M., TAM, W., CHAN, W. C., INGHIRAMI, G. & D'AMORE, F. 2019. Myeloproliferative and lymphoproliferative malignancies occurring in the same patient: a nationwide discovery cohort. *Haematologica*.
- HU, L., LI, Z., CHENG, J., RAO, Q., GONG, W., LIU, M., SHI, Y. G., ZHU, J., WANG, P. & XU, Y. 2013. Crystal structure of TET2-DNA complex: insight into TET-mediated 5mC oxidation. *Cell*, 155, 1545-55.
- JAISWAL, S., FONTANILLAS, P., FLANNICK, J., MANNING, A., GRAUMAN, P. V., MAR, B. G., LINDSLEY, R. C., MERMEL, C. H., BURTT, N., CHAVEZ, A., HIGGINS, J. M., MOLTCHANOV, V., KUO, F. C., KLUK, M. J., HENDERSON, B., KINNUNEN, L., KOISTINEN, H. A., LADENVALL, C.,

- GETZ, G., CORREA, A., BANAHAN, B. F., GABRIEL, S., KATHIRESAN, S., STRINGHAM, H. M., MCCARTHY, M. I., BOEHNKE, M., TUOMILEHTO, J., HAIMAN, C., GROOP, L., ATZMON, G., WILSON, J. G., NEUBERG, D., ALTSHULER, D. & EBERT, B. L. 2014. Age-related clonal hematopoiesis associated with adverse outcomes. *N Engl J Med*, 371, 2488-98.
- KATAOKA, K. & OGAWA, S. 2016. Variegated RHOA mutations in human cancers. *Exp Hematol*, 44, 1123-1129.
- KOMMALAPATI, A., TELLA, S. H., GO, R. S., BENNANI, N. N. & GOYAL, G. 2019. A population-based analysis of second primary malignancies in T-cell neoplasms. *British journal of haematology*, 185, 338-342.
- KOPANOS, C., TSIOLKAS, V., KOURIS, A., CHAPPLE, C. E., ALBARCA AGUILERA, M., MEYER, R. & MASSOURAS, A. 2018. VarSome: the human genomic variant search engine. *Bioinformatics*, 35, 1978-1980.
- KYRIAKOU, C., CANALS, C., GOLDSTONE, A., CABALLERO, D., METZNER, B., KOBBE, G., KOLB, H. J., KIENAST, J., REIMER, P., FINKE, J., OBERG, G., HUNTER, A., THEORIN, N., SUREDA, A., SCHMITZ, N., OUTCOME-LYMPHOMA WORKING PARTY OF THE EUROPEAN GROUP FOR, B. & MARROW, T. 2008. High-dose therapy and autologous stem-cell transplantation in angioimmunoblastic lymphoma: complete remission at transplantation is the major determinant of Outcome-Lymphoma Working Party of the European Group for Blood and Marrow Transplantation. *J Clin Oncol*, 26, 218-24.
- LANGEMEIJER, S. M., KUIPER, R. P., BERENDS, M., KNOPS, R., ASLANYAN, M. G., MASSOP, M., STEVENS-LINDERS, E., VAN HOOGEN, P., VAN KESSEL, A. G., RAYMAKERS, R. A., KAMPING, E. J., VERHOEF, G. E., VERBURGH, E., HAGEMEIJER, A., VANDENBERGHE, P., DE WITTE, T., VAN DER REIJDEN, B. A. & JANSEN, J. H. 2009. Acquired mutations in TET2 are common in myelodysplastic syndromes. *Nat Genet*, 41, 838-42.
- LEMONNIER, F., COURONNE, L., PARRENS, M., JAIS, J. P., TRAVERT, M., LAMANT, L., TOURNILLAC, O., ROUSSET, T., FABIANI, B., CAIRNS, R. A., MAK, T., BASTARD, C., BERNARD, O. A., DE LEVAL, L. & GAULARD, P. 2012. Recurrent TET2 mutations in peripheral T-cell lymphomas correlate with TFH-like features and adverse clinical parameters. *Blood*, 120, 1466-9.
- LEWIS, N. E., PETROVA-DRUS, K., HUET, S., EPSTEIN-PETERSON, Z. D., GAO, Q., SIGLER, A. E., BAIK, J., OZKAYA, N., MOSKOWITZ, A. J., KUMAR, A., HORWITZ, S. M., ZHANG, Y., ARCILA, M. E., LEVINE, R. L., ROSHAL, M., DOGAN, A. & XIAO, W. 2020. Clonal hematopoiesis in angioimmunoblastic T-cell lymphoma with divergent evolution to myeloid neoplasms. *Blood Adv*, 4, 2261-2271.

- LEY, T. J., DING, L., WALTER, M. J., MCLELLAN, M. D., LAMPRECHT, T., LARSON, D. E., KANDOTH, C., PAYTON, J. E., BATY, J., WELCH, J., HARRIS, C. C., LICHTI, C. F., TOWNSEND, R. R., FULTON, R. S., DOOLING, D. J., KOBOLDT, D. C., SCHMIDT, H., ZHANG, Q., OSBORNE, J. R., LIN, L., O'LAUGHLIN, M., MCMICHAEL, J. F., DELEHAUNTY, K. D., MCGRATH, S. D., FULTON, L. A., MAGRINI, V. J., VICKERY, T. L., HUNDAL, J., COOK, L. L., CONYERS, J. J., SWIFT, G. W., REED, J. P., ALLDREDGE, P. A., WYLIE, T., WALKER, J., KALICKI, J., WATSON, M. A., HEATH, S., SHANNON, W. D., VARGHESE, N., NAGARAJAN, R., WESTERVELT, P., TOMASSON, M. H., LINK, D. C., GRAUBERT, T. A., DIPERSIO, J. F., MARDIS, E. R. & WILSON, R. K. 2010. DNMT3A mutations in acute myeloid leukemia. *N Engl J Med*, 363, 2424-33.
- LI, W., MORRONE, K., KAMBHAMPATI, S., WILL, B., STEIDL, U. & VERMA, A. 2016. Thrombocytopenia in MDS: epidemiology, mechanisms, clinical consequences and novel therapeutic strategies. *Leukemia*, 30, 536-544.
- MORAN-CRUSIO, K., REAVIE, L., SHIH, A., ABDEL-WAHAB, O., NDIAYE-LOBRY, D., LOBRY, C., FIGUEROA, M. E., VASANTHAKUMAR, A., PATEL, J., ZHAO, X., PERNA, F., PANDEY, S., MADZO, J., SONG, C., DAI, Q., HE, C., IBRAHIM, S., BERAN, M., ZAVADIL, J., NIMER, S. D., MELNICK, A., GODLEY, L. A., AIFANTIS, I. & LEVINE, R. L. 2011. Tet2 loss leads to increased hematopoietic stem cell self-renewal and myeloid transformation. *Cancer Cell*, 20, 11-24.
- MOSALPURIA, K., BOCIEK, R. G. & VOSE, J. M. 2014. Angioimmunoblastic T-cell lymphoma management. *Semin Hematol*, 51, 52-8.
- MOURAD, N., MOUNIER, N., BRIERE, J., RAFFOUX, E., DELMER, A., FELLER, A., MEIJER, C. J., EMILE, J. F., BOUABDALLAH, R., BOSLY, A., DIEBOLD, J., HAIOUN, C., COIFFIER, B., GISSELBRECHT, C., GAULARD, P. & GROUPE D'ETUDE DES LYMPHOMES DE, L. A. 2008. Clinical, biologic, and pathologic features in 157 patients with angioimmunoblastic T-cell lymphoma treated within the Groupe d'Etude des Lymphomes de l'Adulte (GELA) trials. *Blood*, 111, 4463-70.
- NAGATA, Y., KONTANI, K., ENAMI, T., KATAOKA, K., ISHII, R., TOTOKI, Y., KATAOKA, T. R., HIRATA, M., AOKI, K., NAKANO, K., KITANAKA, A., SAKATA-YANAGIMOTO, M., EGAMI, S., SHIRAISHI, Y., CHIBA, K., TANAKA, H., SHIOZAWA, Y., YOSHIZATO, T., SUZUKI, H., KON, A., YOSHIDA, K., SATO, Y., SATO-OTSUBO, A., SANADA, M., MUNAKATA, W., NAKAMURA, H., HAMA, N., MIYANO, S., NUREKI, O., SHIBATA, T., HAGA, H., SHIMODA, K., KATADA, T., CHIBA, S., WATANABE, T. & OGAWA, S. 2016. Variegated RHOA mutations in adult T-cell leukemia/lymphoma. *Blood*, 127, 596-604.
- NAKAJIMA, H. & KUNIMOTO, H. 2014. TET2 as an epigenetic master regulator for normal and malignant hematopoiesis. *Cancer Sci*, 105, 1093-9.

- O'HAYRE, M., INOUE, A., KUFAREVA, I., WANG, Z., MIKELIS, C. M., DRUMMOND, R. A., AVINO, S., FINKEL, K., KALIM, K. W., DIPASQUALE, G., GUO, F., AOKI, J., ZHENG, Y., LIONAKIS, M. S., MOLINOLO, A. A. & GUTKIND, J. S. 2016. Inactivating mutations in GNA13 and RHOA in Burkitt's lymphoma and diffuse large B-cell lymphoma: a tumor suppressor function for the Galpha13/RhoA axis in B cells. *Oncogene*, 35, 3771-80.
- ORGANIZATION, W. H. 2011. Haemoglobin concentrations for the diagnosis of anaemia and assessment of severity. World Health Organization.
- PALOMERO, T., COURONNE, L., KHIABANIAN, H., KIM, M. Y., AMBESI-IMPIOMBATO, A., PEREZ-GARCIA, A., CARPENTER, Z., ABATE, F., ALLEGRETTA, M., HAYDU, J. E., JIANG, X., LOSSOS, I. S., NICOLAS, C., BALBIN, M., BASTARD, C., BHAGAT, G., PIRIS, M. A., CAMPO, E., BERNARD, O. A., RABADAN, R. & FERRANDO, A. A. 2014. Recurrent mutations in epigenetic regulators, RHOA and FYN kinase in peripheral T cell lymphomas. *Nat Genet*, 46, 166-70.
- PAPAEEMMANUIL, E., GERSTUNG, M., MALCOVATI, L., TAURO, S., GUNDEM, G., VAN LOO, P., YOON, C. J., ELLIS, P., WEDGE, D. C., PELLAGATTI, A., SHLIEN, A., GROVES, M. J., FORBES, S. A., RAINE, K., HINTON, J., MUDIE, L. J., MCLAREN, S., HARDY, C., LATIMER, C., DELLA PORTA, M. G., O'MEARA, S., AMBAGLIO, I., GALLI, A., BUTLER, A. P., WALLDIN, G., TEAGUE, J. W., QUEK, L., STERNBERG, A., GAMBACORTI-PASSERINI, C., CROSS, N. C., GREEN, A. R., BOULTWOOD, J., VYAS, P., HELLSTROM-LINDBERG, E., BOWEN, D., CAZZOLA, M., STRATTON, M. R., CAMPBELL, P. J. & CHRONIC MYELOID DISORDERS WORKING GROUP OF THE INTERNATIONAL CANCER GENOME, C. 2013. Clinical and biological implications of driver mutations in myelodysplastic syndromes. *Blood*, 122, 3616-27; quiz 3699.
- QUIVORON, C., COURONNE, L., DELLA VALLE, V., LOPEZ, C. K., PLO, I., WAGNER-BALLON, O., DO CRUZEIRO, M., DELHOMMEAU, F., ARNULF, B., STERN, M. H., GODLEY, L., OPOLON, P., TILLY, H., SOLARY, E., DUFFOURD, Y., DESSEN, P., MERLE-BERAL, H., NGUYEN-KHAC, F., FONTENAY, M., VAINCHENKER, W., BASTARD, C., MERCHER, T. & BERNARD, O. A. 2011. TET2 inactivation results in pleiotropic hematopoietic abnormalities in mouse and is a recurrent event during human lymphomagenesis. *Cancer Cell*, 20, 25-38.
- ROHR, J., GUO, S., HUO, J., BOUSKA, A., LACHEL, C., LI, Y., SIMONE, P. D., ZHANG, W., GONG, Q., WANG, C., CANNON, A., HEAVICAN, T., MOTTOK, A., HUNG, S., ROSENWALD, A., GASCOYNE, R., FU, K., GREINER, T. C., WEISENBURGER, D. D., VOSE, J. M., STAUDT, L. M., XIAO, W., BORGSTAHL, G. E., DAVIS, S., STEIDL, C., MCKEITHAN, T., IQBAL, J. & CHAN, W. C. 2016. Recurrent activating mutations of CD28 in peripheral T-cell lymphomas. *Leukemia*, 30, 1062-70.

- SAKATA-YANAGIMOTO, M., ENAMI, T., YOSHIDA, K., SHIRAISHI, Y., ISHII, R., MIYAKE, Y., MUTO, H., TSUYAMA, N., SATO-OTSUBO, A., OKUNO, Y., SAKATA, S., KAMADA, Y., NAKAMOTO-MATSUBARA, R., TRAN, N. B., IZUTSU, K., SATO, Y., OHTA, Y., FURUTA, J., SHIMIZU, S., KOMENO, T., SATO, Y., ITO, T., NOGUCHI, M., NOGUCHI, E., SANADA, M., CHIBA, K., TANAKA, H., SUZUKAWA, K., NANMOKU, T., HASEGAWA, Y., NUREKI, O., MIYANO, S., NAKAMURA, N., TAKEUCHI, K., OGAWA, S. & CHIBA, S. 2014. Somatic RHOA mutation in angioimmunoblastic T cell lymphoma. *Nat Genet*, 46, 171-5.
- SCHWARTZ, F. H., CAI, Q., FELLMANN, E., HARTMANN, S., MÄYRÄNPÄÄ, M. I., KARJALAINEN-LINDSBERG, M. L., SUNDSTRÖM, C., SCHOLTYSIK, R., HANSMANN, M. L. & KÜPPERS, R. 2017. TET2 mutations in B cells of patients affected by angioimmunoblastic T-cell lymphoma. *The Journal of pathology*, 242, 129-133.
- SPERLING, A. S., GIBSON, C. J. & EBERT, B. L. 2017. The genetics of myelodysplastic syndrome: from clonal haematopoiesis to secondary leukaemia. *Nat Rev Cancer*, 17, 5-19.
- SRINIVASAN, M., SEDMAK, D. & JEWELL, S. 2002. Effect of fixatives and tissue processing on the content and integrity of nucleic acids. *Am J Pathol*, 161, 1961-71.
- STEENSMA, D. P., BEJAR, R., JAISWAL, S., LINDSLEY, R. C., SEKERES, M. A., HASSERJIAN, R. P. & EBERT, B. L. 2015. Clonal hematopoiesis of indeterminate potential and its distinction from myelodysplastic syndromes. *Blood*, 126, 9-16.
- STEIN, E. M., DINARDO, C. D., POLLYEA, D. A., FATHI, A. T., ROBOZ, G. J., ALTMAN, J. K., STONE, R. M., DEANGELO, D. J., LEVINE, R. L., FLINN, I. W., KANTARJIAN, H. M., COLLINS, R., PATEL, M. R., FRANKEL, A. E., STEIN, A., SEKERES, M. A., SWORDS, R. T., MEDEIROS, B. C., WILLEKENS, C., VYAS, P., TOSOLINI, A., XU, Q., KNIGHT, R. D., YEN, K. E., AGRESTA, S., DE BOTTON, S. & TALLMAN, M. S. 2017. Enasidenib in mutant IDH2 relapsed or refractory acute myeloid leukemia. *Blood*, 130, 722-731.
- STEINHILBER, J., MEDERAKE, M., BONZHEIM, I., SERINSOZ-LINKE, E., MULLER, I., FALLIER-BECKER, P., LEMONNIER, F., GAULARD, P., FEND, F. & QUINTANILLA-MARTINEZ, L. 2019. The pathological features of angioimmunoblastic T-cell lymphomas with IDH2(R172) mutations. *Mod Pathol*.
- STONE, M. J. Thomas Hodgkin: medical immortal and uncompromising idealist. *Baylor University Medical Center Proceedings*, 2005. Taylor & Francis, 368-375.

- SWERDLOW, S., CAMPO, E., HARRIS, N. L., JAFFE, E., PILERI, S., STEIN, H., THIELE, J., ARBER, D., HASSERJIAN, R. & LE BEAU, M. 2017. WHO classification of tumours of haematopoietic and lymphoid tissues (Revised 4th edition). *IARC: Lyon*, 421.
- TOKUNAGA, T., SHIMADA, K., YAMAMOTO, K., CHIHARA, D., ICHIHASHI, T., OSHIMA, R., TANIMOTO, M., IWASAKI, T., ISODA, A., SAKAI, A., KOBAYASHI, H., KITAMURA, K., MATSUE, K., TANIWAKI, M., TAMASHIMA, S., SABURI, Y., MASUNARI, T., NAOE, T., NAKAMURA, S. & KINOSHITA, T. 2012. Retrospective analysis of prognostic factors for angioimmunoblastic T-cell lymphoma: a multicenter cooperative study in Japan. *Blood*, 119, 2837-43.
- UNTERGASSER, A., CUTCUTACHE, I., KORESSAAR, T., YE, J., FAIRCLOTH, B. C., REMM, M. & ROZEN, S. G. 2012. Primer3--new capabilities and interfaces. *Nucleic Acids Res*, 40, e115.
- VALLOIS, D., DOBAY, M. P., MORIN, R. D., LEMONNIER, F., MISSIAGLIA, E., JUILLAND, M., IWASZKIEWICZ, J., FATACCIOLI, V., BISIG, B., ROBERTI, A., GREWAL, J., BRUNEAU, J., FABIANI, B., MARTIN, A., BONNET, C., MICHIELIN, O., JAIS, J. P., FIGEAC, M., BERNARD, O. A., DELORENZI, M., HAIOUN, C., TOURNILHAC, O., THOME, M., GASCOYNE, R. D., GAULARD, P. & DE LEVAL, L. 2016. Activating mutations in genes related to TCR signaling in angioimmunoblastic and other follicular helper T-cell-derived lymphomas. *Blood*, 128, 1490-502.
- VOSE, J., ARMITAGE, J., WEISENBURGER, D. & INTERNATIONAL, T. C. L. P. 2008. International peripheral T-cell and natural killer/T-cell lymphoma study: pathology findings and clinical outcomes. *J Clin Oncol*, 26, 4124-30.
- WANG, M., ZHANG, S., CHUANG, S.-S., ASHTON-KEY, M., OCHOA, E., BOLLI, N., VASSILIOU, G., GAO, Z. & DU, M.-Q. 2017. Angioimmunoblastic T cell lymphoma: novel molecular insights by mutation profiling. *Oncotarget*, 8, 17763.
- YAN, H., PARSONS, D. W., JIN, G., MCLENDON, R., RASHEED, B. A., YUAN, W., KOS, I., BATINIC-HABERLE, I., JONES, S., RIGGINS, G. J., FRIEDMAN, H., FRIEDMAN, A., REARDON, D., HERNDON, J., KINZLER, K. W., VELCULESCU, V. E., VOGELSTEIN, B. & BIGNER, D. D. 2009. IDH1 and IDH2 mutations in gliomas. *N Engl J Med*, 360, 765-73.
- YANG, L., RAU, R. & GOODELL, M. A. 2015. DNMT3A in haematological malignancies. *Nat Rev Cancer*, 15, 152-65.
- YOO, H. Y., SUNG, M. K., LEE, S. H., KIM, S., LEE, H., PARK, S., KIM, S. C., LEE, B., RHO, K., LEE, J. E., CHO, K. H., KIM, W., JU, H., KIM, J., KIM, S. J., KIM, W. S., LEE, S. & KO, Y. H. 2014. A recurrent inactivating

mutation in RHOA GTPase in angioimmunoblastic T cell lymphoma. *Nat Genet*, 46, 371-5.

YOU, J. S. & JONES, P. A. 2012. Cancer genetics and epigenetics: two sides of the same coin? *Cancer Cell*, 22, 9-20.

7 Declaration of Authorship

This project was conducted at the Institute of Pathology and Neuropathology at the University Hospital of Tübingen (medical director: **Prof. Dr. Falko Fend**) under supervision of **Prof. Dr. Leticia Quintanilla-Fend**.

The objective and experimental setup were outlined by **Prof. Dr. Leticia Quintanilla-Fend** and **Dr. Irina Bonzheim**.

The experiments and analysis were conducted by me, unless stated otherwise, in close collaboration with **Dr. Irina Bonzheim** and **Vanessa Borgmann**.

Microscopical pictures were taken together with **Ivonne Montes**.

I hereby certify that this thesis has been composed by me and is based on my own work, unless stated otherwise. No other person's work has been used without due acknowledgements in this thesis. All references and verbatim extracts have been quoted, and all sources of information, including graphs and data sets, have been specifically acknowledged.

Tübingen, 7th March 2021

Lennart Harland

8 Acknowledgements

I like to express my gratitude to everyone, who was involved in this thesis and helped me throughout the whole project; however, I like to express special gratitude to some people in particular.

I would first like to thank **Prof. Dr. Leticia Quintanilla-Fend** for her supervision during the project. I consider myself fortunate collaborating with such an expert in the field. She never failed to propel the project and responded even late at night, which made me feel very much appreciated as a student.

Moreover, I am grateful to the medical director, **Prof. Dr. Falko Fend**, for the opportunity to conduct the experiments at the institute. His invaluable comments on the project were undeniably constructive as they opened new perspectives.

I would like to express special gratitude to **Vanessa Borgmann** and **Dr. Irina Bonzheim** for their great impact on the project. They contributed significantly to every single aspect of this work. I am thankful for your commitment, as both of you found time even during stressful days.

My appreciation also extends to **Franziska Mihalik**, **Rebecca Braun**, **Sema Colak** and **Esther Kohler** for their constant help during lab work. I was lucky to conduct my experiments in such a pleasant environment.

I also want to thank **Ivonne Montes**, **Dr. Dominik Nann**, and the doctoral students for their support.

Finally, I want to thank my family starting with my beloved wife, **Katrin Harland**. Your never-ending commitment during the project is inspiring. For this and a lot more, I want to thank you from the bottom of my heart.

Last but not least, I dedicate this thesis to my parents, **Dr. Thomas** and **Kathrin Fiedler**. Without your love, wisdom, and endless support none of this would have been possible.